Geoderma 247–248 (2015) 73–87

Contents lists available at ScienceDirect

Geoderma

journal homepage: www.elsevier.com/locate/geoderma

Long-term controls on soil organic carbon with depth and time: A case study from the Cowlitz River Chronosequence, WA USA

Corey R. Lawrence [a,*], Jennifer W. Harden [a], Xiaomei Xu [b], Marjorie S. Schulz [a], Susan E. Trumbore [b,c]

[a] U.S. Geological Survey, Menlo Park, CA USA
[b] University of California, Irvine, CA USA
[c] Max Planck Institute of Biogeochemistry, Jena, Germany

ARTICLE INFO

Article history:
Received 8 October 2014
Received in revised form 11 February 2015
Accepted 15 February 2015
Available online 3 March 2015

Keywords:
Carbon
Soils
Pedogenesis
Mineralogy
Organo-metal
Radiocarbon

ABSTRACT

Over timescales of soil development (millennia), the capacity of soils to stabilize soil organic carbon (SOC) is linked to soil development through changes in soil mineralogy and other soil properties. In this study, an extensive dataset of soil profile chemistry and mineralogy is compiled from the Cowlitz River Chronosequence (CRC), WA USA. The CRC soils range in age from 0.25 to 1200 kyr, spanning a developmental gradient encompassing clear changes in soil mineralogy, chemistry, and surface area. Comparison of these and other metrics of soil development with SOC properties reveal several relationships that may be diagnostic of the long-term coupling of soil development and C cycling. Specifically, SOC content was significantly correlated with sodium pyrophosphate extractable metals emphasizing the relevance of organo-metal complexes in volcanic soils. The depth distributions of organo-metals and other secondary weathering products, including the kaolin and short-range order (SRO) minerals, support the so-called "binary composition" of volcanic soils. The formation of organo-metal complexes limits the accumulation of secondary minerals in shallow soils, whereas in deep soils with lower SOC content, secondary minerals accumulate. In the CRC soils, secondary minerals formed in deep soils (below 50 cm) including smectite, allophane, Fe-oxides and dominated by the kaolin mineral halloysite. The abundance of halloysite was significantly correlated with bulk soil surface area and ^{14}C content (a proxy for the mean age of SOC), implying enhanced stability of C in deep soils. Allophane, an SRO mineral commonly associated with SOC storage, was not correlated with SOC content or ^{14}C values in CRC soils. We propose conceptual framework to describe these observations based on a general understanding of pedogenesis in volcanic soils, where SOC cycling is coupled with soil development through the formation of and fate of organo-metal or other mobile weathering products. This framework highlights interactions between SOC and soil development, which may be applicable to other soils where organic inputs interact with the products of chemical weathering.

1. Introduction

Soil organic matter is the largest terrestrial pool of carbon (C), accounting for more than three times the mass of C in the atmosphere (Batjes, 1996; Tarnocai et al., 2009). Uncertainty surrounding the fate of soil organic C (SOC) in response to global change reduces confidence in predictions of the feedback of soils on future climate. In particular, factors controlling SOC turnover in deep soils (>50 cm) are increasingly recognized as significant to the overall SOC storage and stability (Fontaine et al., 2007; Rumpel and Kögel-Knabner, 2010). Carbon stabilized at depths >20 cm accounts for more than 50% of the total organic C stocks in several ecosystem types (Jobbagy and Jackson, 2000), and deep SOC is often considered to be recalcitrant and/or inaccessible to microbial degradation (Rumpel and Kögel-Knabner, 2010). However, radiocarbon based estimates of SOC turnover times suggest that seemingly recalcitrant C pools can turnover quickly (Amelung et al., 2008; Cusack et al., 2012; Marschner et al., 2008; Schmidt et al., 2011). Similarly, old and/or deep C may be readily decomposed under favorable environmental conditions (Schimel et al., 2011). These observations highlight a need to understand the mechanisms leading to SOC stabilization in deep soils and the processes that couple shallow and deep soil environments.

Soil organic C stabilization is generally partitioned between physical protection and chemical mechanisms (Eusterhues et al., 2003; Kögel-Knabner et al., 2008; von Lützow and Kögel-Knabner, 2010; Oades, 1988; Sollins et al., 1996). Physical stabilization of SOC is often linked to the formation of soil structure (i.e., aggregates) that may limit the diffusion of enzymes and/or catabolites (Blanco-Canqui and Lal, 2004; Oades, 1988; Rasmussen et al., 2005; Six et al., 2000, 2002), but may also refer to physical state, such as frozen SOC in permafrost

* Corresponding author at: U.S. Geological Survey, MS 980, Box 25046, Federal Center, Denver, CO 80225, USA.
E-mail address: clawrence@usgs.gov (C.R. Lawrence).

http://dx.doi.org/10.1016/j.geoderma.2015.02.005

soils (Harden et al., 2012). Chemical stabilization results from adsorption of SOC to mineral surfaces or from aqueous complexation of dissolved organics with mineral weathering products such as dissolved Fe and Al (Eusterhues et al., 2003; Kaiser and Guggenberger, 2000; Kalbitz and Kaiser, 2008; Mikutta et al., 2005; Schwesig et al., 2003). The stability of some SOC compounds may also result from chemical recalcitrance or energetic limitations associated with the degradation of complex organic compounds. However, chemical recalcitrance is increasingly viewed as a relative rather than absolute property of SOC (von Lützow et al., 2006) and there is little evidence that such intrinsic properties are important controls on SOC over timescales of decades to millennia (Marschner et al., 2008; Schmidt et al., 2011).

As soil biogeochemical properties evolve during pedogenesis, the dominant mechanisms leading to stability of SOC may change. These temporal changes in soil properties are often slow and non-reversible, proceeding along a trajectory set by the antecedent conditions and soil forming factors, including climate, organisms, parent material, topography and the duration of soil development (Jenny, 1994). Over the course of soil development, chemical weathering reactions lead to shifts in the composition of soil mineralogy (Chorover et al., 2004; Huggett, 1998; White et al., 1996, 2008). This evolution of soil mineralogy drives changes in other soil properties influencing SOC stabilization. Correspondingly, the relative importance of various mechanisms of SOM physical and chemical protection change through time as a function of soil mineralogy (Lilienfein et al., 2003; Masiello et al., 2004; Torn et al., 1997). Temporally dynamic soil properties include the depth distribution of weathering products (e.g., dissolved Fe and Al), which can form organo-metal (i.e., metal-humus) complexes; changes in reactive mineral surface area and bulk soil porosity; soil hydrologic fluxes, which control the transport of DOM and weathering products; physical changes involving aggregation, porosity, density, and soil strength. The chemistry, mineralogy and self-organization (i.e., formation of soil horizons) of soils allow for classification of soil-type. Given some knowledge of soil forming factors, changes in soil properties during development may be predicted (Jenny, 1994).

Trajectories of soil development, including progressive changes in soil mineralogy and associated properties, have often been quantified using soil chronosequences (Harden, 1982; Lilienfein et al., 2003; Masiello et al., 2004; Torn et al., 1997; Walker et al., 2010). These, along with other studies, have shaped our understanding of the progressive evolution of soil mineralogy and its influence on SOC storage and stability (Baldock and Skjemstad, 2000). In a very general sense, primary minerals weather to form secondary minerals including Fe-oxides (e.g., ferrihydrite and goethite), Al-oxyhydroxides (e.g., gibbsite), short-range order (SRO) or noncrystalline minerals (e.g., allophane and imogolite) and phyllosilicates including halloysite and kaolinite (Chadwick and Chorover, 2001; Jackson et al., 1948; Merrill, 1897). The composition and abundance of secondary minerals are a dominant control on the evolution of other soil properties. For example, in some weathering environments, SRO minerals are formed that are characterized by large and highly reactive surface area resulting in an exceptional capacity to sequester C (Chorover et al., 2004; Kleber et al., 2005; Mikutta et al., 2005; Torn et al., 1997). With additional weathering, SRO minerals may be converted to more crystalline kaolin minerals, resulting in a reduction of mineral surface area and C storage (Parfitt, 2009; Torn et al., 1997). Although typically slow (i.e., millenia), the dynamics of secondary mineral formation (and thus C storage) may change more quickly when soil pedogenic thresholds, such as increased colloidal flocculation and decreased permeability, are crossed (McFadden and Weldon, 1987). Quantification of these trajectories and thresholds in soil development should improve our understanding of SOC cycling with depth and time and will likely form the basis for mechanistic models aimed at a more accurate representation of deep, slow cycling SOC.

Soil development also produces mobile weathering products that may interact with SOC, resulting in feedbacks on SOC cycling and soil mineralogy (e.g., Lawrence et al., 2014). For example, the flux of dissolved organic C (DOC) is known to be an important source of modern C to deep soil horizons (Guggenberger and Kaiser, 2003; Kaiser and Kalbitz, 2012; Kalbitz et al., 2000; Sanderman and Amundson, 2009; Sanderman et al., 2008), but such inputs of fresh C have also shown to destabilize deep SOC stocks (Fontaine et al., 2007). Relatedly, dissolved weathering products, including Al^{3+} and Fe^{2+}, may react with organic ligands to form organo-metal complexes (Ganor et al., 2009; Jones, 1998; Matus et al., 2006; Mikutta et al., 2006; Pena-Ramirez et al., 2009; Percival et al., 2000; Sollins et al., 1996; van Hees et al., 2000). These complexes are known to control Al solubility in soils (Berggren and Mulder, 1995; Dijkstra and Fitzhugh, 2003) and when incorporated in a reactive transport based model of soil weathering, the stability of the organo-metal complexes were shown to influence the depth and extent of secondary mineral precipitation (Lawrence et al., 2014). Several studies have also demonstrated a strong significant correlation between sodium pyrophosphate extractable Al and total soil C (Masiello et al., 2004; Percival et al., 2000; Wada and Higashi, 1976; Wagai et al., 2011), implying a widespread connection between organo-metal complexation and long-term storage and stability of SOC. However, the appropriateness of these techniques as a proxy for organo-complexed metals has been questioned (Kaiser and Zech, 1996; Parfitt and Childs, 1988) and the mechanisms linking these reactions to soil C storage are not well understood.

Given the recognition of soil physical and chemical properties as important controls on SOC cycling through space and time, there is a growing need to include these edaphic soil properties in process-based models (Schmidt et al., 2011; Trumbore and Czimczik, 2008). In particular, greater attention must be given to how controls on C turnover vary with depth (Rumpel and Kögel-Knabner, 2010) including interactions of organic inputs with the products of chemical weathering (Lawrence et al., 2014). The goal of this study is to advance a framework for linking temporal (e.g., millennial scale) changes in soil development with the storage and stability of SOC, including depth-dependent evolution of soil mineral profiles and stabilization of SOC through organic-mineral and organic-metal associations.

2. Methods

2.1. Site description

The Cowlitz River is located in southwestern Washington State, USA and flows west from Mount Rainier toward its confluence with the Columbia River (Supplemental Fig. 1). During the Pleistocene, glaciers repeatedly expanded into the Cowlitz River Valley, carving terraces into previously deposited gravel and sand outwash materials. In most cases, these deposits were subsequently covered with a thick (0.5 to 5 m) layer of silt-textured loess, blown in from outwash plains (Dethier, 1988). Soils forming in terraces of the Cowlitz River have been linked to four glacial deposits including Wisconsin Evans Creek Drift, pre-Wisconsin Hayden Creek Drift, late Pleistocene Wingate Hill Drift, and middle or late Pleistocene Logan Hill Formation (Bethel, 1982; Dethier, 1988). Sandy-gravel outwash plains formed during these glacial periods. Sediment transported from the glacial terminus was deposited as broad sheets through which the present day Cowlitz River channel flows. In total, the Cowlitz River Chronosequence (CRC) is comprised of 10 loess-mantled gravel terraces, differing primarily in length of time since soil development was initiated (Dethier, 1988). The CRC soils were formed from sediments of similar mineralogical composition and depositional environments, implying relatively homogenous soil parent material across the chronosequence. Parent material consisted primarily of basalt and andesite gravel mixed with tephra and silt-sized volcanic sediments of the loess inputs. Although it is likely that some additional loess inputs were superimposed on existing soils during each successive glacial event, there is no evidence that such inputs were great enough to reset soil development. Dethier (1988)

suggested that over long-timescales the input of additional loess to existing soils could be considered constant, with the exception of the 24 kyr soil, which contained a fine-grained layer rich in glassy dacite debris. These small but consistent inputs of loess likely contributed to soil development and geochemical heterogeneity but quantification of this influence is beyond the scope of this study.

The generally flat (<2°) soil terraces are best preserved in the region between Toledo and Mayfield, WA and are separated from one another by steep slope transitions, occurring with 100 to 200 m of elevation change. Although the absolute age is uncertain for many of the older terraces, a relative stratigraphy of terraces has been established and ages of individual terraces have been estimated to range from 0.25 to 1200 kyr (Table 1). The original measurements of the CRC terrace soils indicated clay content, clay films, dithionite extractable Fe_d and Al_d, the depth to unweathered material, and rubification all increased with estimated soil age (Dethier, 1988). The concentrations of more mobile oxides including Ca, Na, and K as well as soil pH (which varies from 5.00 to 6.21), decrease with increasing soil age (Supplemental Table 1). From calculated metrics of soil development (i.e., Harden and Taylor, 1983), the observed patterns correspond to a distinct pattern of increasing soil development, which is well correlated with the assumed age stratigraphy (Dethier, 1988). This finding strongly supports use of the CRC to better understand the relationship between soil development and long-term soil C cycling.

The Cowlitz River region is characterized as a maritime climate, with cool wet winter and warm dry summers. The mean annual temperature for the nearby town of Toledo, WA was 10.6 °C (NOAA National Climatic Data Center, 1981–2010) and the mean annual precipitation ranged from 1200 mm near Chehalis, WA to 1432 mm near Mayfield, WA (NOAA National Climatic Data Center, 1981–2010). At the time European settlers arrived in the Cowlitz River area during the mid 19th century, terrace plant communities consisted of prairie vegetation and some old-growth coniferous forests (Soils Survey of Lewis Country area, Washington, 1987). At the time of sampling (analyses reported in this study were performed on archived samples collected from 1979 to 1981), most study sites were dominated by second-growth forests consisting of Douglas fir (*Pseudotsuga mezeseii*), fir (*Abies sp.*), hemlock (*Tsuga heterophylla*) and red cedar (*Thuja plicata*) mixed with alder (*Alnus rubra*), maple (*Acer marophyllum*) and willow (*Salix* sp.) (Dethier, 1988). During the timescales of soil development at the CRC, vegetation communities have likely varied as result of natural succession and fluctuations in climate and land use. The chemical history recorded in chronosequence soils reflects site-specific history based on local factors such as land use and, in older soils, periods of variability not recorded in the youngest soils. In long-term chronosequence studies such as this, it is difficult to quantify site-specific disturbances (i.e., land use variations, superimposed loess deposition and erosion), which may influence soils of the chronosequence disproportionately. Moreover, in the absence of disturbances that reset or completely halt soil development, minor changes (e.g., small but continuous loess inputs) must be viewed as a natural component of the pedogenic processes.

Table 1
Soil of the Cowlitz River Chronosequence (CRC). Samples were collected from 1979 to 1981.
Age estimates and site numbers are from Dethier (1988).

Quaternary deposit	Age range (kyr)	Best age (kyr)
Late Holocene alluvium	<0.25	0.25
Latest Pleistocene outwash	10.0–12.0	11
Evans Creek Drift	–	–
– *Late outwash*	14.0	14
– *Early outwash*	24.0	24
Pre-Evans Creek outwash	40–70	60
Hayden Creek Drift	–	–
– *Late outwash*	65–170	150
– *Middle outwash*	130–280	225
– *Early outwash*	240–340	300
Wingate Hill Drift and outwash	300–600	500
Logan Hill Formation	630–1600	1200

2.2. Sample collection and processing

Dethier (1988) collected soil samples from outcrops (soils <24 kyr) or from machine-excavated soil pits. Sampling depths ranged from 1.2 to 3 m and samples were collected by horizon. However, complete soil profiles were not sampled in older soils that exceeded 3 m depth (Dethier, 1988). After collection, samples were sieved to 2 mm and several physical and chemical analyses were completed including total organic C and nitrogen (N), textural analysis; and major oxide concentrations. These data are reported in Dethier (1988). Following this initial work, sample splits were archived in wax coated paper containers at U.S. Geological Survey (USGS) facilities in Menlo Park, CA until 2009, when they were reanalyzed for this study. Except where otherwise noted, data reported here are from modern analyses of these archived samples.

2.3. Carbon and nitrogen analyses

The archived samples were measured for C and N by high-temperature combustion at the USGS laboratories in Menlo Park, CA. Samples were sieved to 2 mm and then ground with a mortar and pestle until they completely passed an 80 μm sieve. The ground samples were then weighed into tin capsules and analyzed using a Carlo Erba NA1500 elemental analyzer (CE Elantech Inc., Lakewood, NJ[1]). In order to verify that soil C content had not changed during the archiving period, C measurements of the archived soils were compared with measurements made on the same samples immediately following collection (~30 years ago). The total mass of C stored in each soil profile was calculated using measured C concentrations (%), which were converted to C density (i.e., mg C g soil^{-1}) using soil bulk density (g cm^{-3}) and sampling depths reported in Dethier (1988). Missing bulk density values were filled using depth dependent linear interpolation between measured values.

The SOC isotopic composition of bulk soils was measured at the W.M. Keck Carbon Cycle Accelerator Mass Spectrometry (AMS) Laboratory of the University of California, Irvine. Prior to analyses, bulk soils were combusted in sealed quartz tubes with CuO at 900 °C for 2 h to convert all organic matter to CO_2. This CO_2 was then purified on a vacuum line and splits of the purified gas were taken for ^{13}C and ^{14}C measurements. The ^{13}C content was measured with a Thermo Scientific Delta Plus XL (Thermo Fisher Scientific, Waltham, MA[1]) isotopic ratio mass spectrometer (IR-MS). The $^{13}C/^{12}C$ of samples was reported relative to the $^{13}C/^{12}C$ of the Pee Dee Belemite (PDB) standard:

$$\delta^{13}C = \left(\frac{{}^{13}C / {}^{12}C_{Sample}}{{}^{13}C / {}^{12}C_{PDB}} - 1 \right) * 1000 \quad (1)$$

The CO_2 split for ^{14}C was graphitized and measured by AMS following the methods of Xu et al. (2007). Radiocarbon data are reported as fraction modern (FM):

$$FM = \left[\frac{\left[\frac{{}^{14}C}{{}^{12}C} \right]_{sample,-25}}{0.95 \left[\frac{{}^{14}C}{{}^{12}C} \right]_{OX1,-19}} \right] \quad (2)$$

where the isotope ratio of a sample was corrected for mass-dependent fractionation by correcting to a common value of $\delta^{13}C$ value of −25‰

[1] Trade names are used for descriptive purposes only and do not constitute endorsement by the U.S. Government.

and normalized to the isotopic ratio of the OX1 standard (Stuiver and Polach, 1977; Trumbore, 2009)

2.4. Quantitative mineralogy, elemental chemistry and surface area

Quantitative mineralogy, total elemental chemistry and bulk soil surface area were measured at the USGS laboratories in Boulder, CO and Menlo Park, CA. Quantitative estimates of soil mineralogy were made using X-ray diffraction (XRD), following the procedure of Eberl (2003). The measured XRD intensities of the sample/standard mixture were compared against the intensity of the internal standard using the RockJock software. Major and selected trace element concentrations were measured from ground samples using X-ray fluorescence spectrometry (XRF). The surface area of bulk soil was measured by BET/nitrogen sorption method using a Micromeritics Tristar II (Micromeritics Instrument Company, Norcross, GA[1]). Cation exchange capacity (CEC) was previously measured for CRC soils prior to archiving (Dethier, 1988) and those results are also included here.

2.5. Elemental mass balance calculations

Element specific chemical depletion factors (CDF) were calculated using the composition of the youngest soils sampled (0.25 kyr) as an approximation of parent material composition. This approach is less than ideal for a chronosequence spanning such a large age gradient but because archive samples were not always collected to the depth of unweathered material, but it provides the most reasonable assessment of long-term elemental changes. The CDF values were calculated following Riebe et al. (2001):

$$CDF_x = \left(1 - \frac{[X]_s [I]_p}{[X]_p [I]_s}\right) \quad (3)$$

where [X] is the concentration of mobile element *x*, and [I] is the concentration of an immobile reference element, *i*. In this case, Ti was used as the immobile reference element and the subscripts *p* and *s* refer to the parent material and soil, respectively. Positive values of CDF_x equate to the fraction of the element, *x*, that has been removed via chemical weathering, whereas negative values correspond to enrichment. Values of CDF_x are equivalent in magnitude but opposite in sign to the commonly reported metric, Tau (Anderson and Dietrich, 2001; Brimhall et al., 1992; Brimhall and Dietrich, 1987; Lawrence et al., 2013).

2.6. Selective mineral dissolutions

Archived samples were subjected to a 2-step sequential chemical extraction to selectively dissolve secondary weathering phases. First, 1 g of sample was weighed into a 50 ml centrifuge tube with 40 ml of sodium pyrophosphate reagent (0.1 M, pH = 10). Samples were shaken for ~16 h and then centrifuged at room temperature for 20 min at approximately 20,000 *g*. After centrifuging, the supernatant was decanted and syringe-filtered through a 0.2 μM graduate membrane filter (Whatman, GD/X, 25 mm diameter) into 50 ml sample tubes. The residual solid sample was dried overnight at ~45 °C. After drying, the residual soils were further extracted with 40 ml of acid ammonium oxalate reagent (0.1 M, pH = 3.0) using a similar procedure, except the ammonium oxalate extraction was performed in the dark using a sealed box (Loeppert and Inskeep, 1996; McKeague and Day, 1966). Concentrations of Al_p, Al_o, Si_o, Fe_p and Fe_o in the filtered solutions were measured by inductively coupled plasma mass spectrometry (ICP-MS) and results were compared with dithionite extracted Al_d and Fe_d concentrations reported in Dethier (1988).

The Al and Fe measured in soil chemical extractions (i.e., sodium pyrophosphate (PP), ammonium oxalate (OX) and dithionite–citrate (DC)) have often been used to estimate the abundances of various secondary mineral classes (Masiello et al., 2004; Parfitt and Childs, 1988; Wagai et al., 2011). However, in some cases these extractions are not as selective as the widely used interpretations suggest (Kaiser and Zech, 1996; Parfitt and Childs, 1988). In light of this prior work, the following interpretations of chemical extraction data (from Wagai et al., 2011) were cautiously applied:

1. The PP extraction was assumed to primarily produce Al_p and Fe_p from dissolution of organo-metal complexes but may also dissolve some (<10%) noncrystalline SRO minerals (e.g., allophane/imogolite) and/or promote limited dispersion of ferrihydrite and goethite colloids.
2. The OX extraction of residual soil (following the PP extraction) was assumed to produce Al_o, Fe_o, and Si_o from the complete dissolution of noncrystalline SRO minerals and ferrihydrite. It was also assumed that the OX extraction partially dissolves magnetite, hematite and gibbsite.
3. The DC method employed by Dethier (1988) was assumed to produce Al_d and Fe_d, from the complete dissolution of organo-metal complexes, ferrihydrite, and goethite as well as partial dissolution of hematite, magnetite and gibbsite.

Several metrics of soil mineralogy and soil development were calculated by combining these selective extraction data. Specifically, the ratio of $Al_p/(Al_p + Al_o)$ provides an estimate of the relative distribution of organo-metal versus noncrystalline SRO weathering products, the ratios Fe_o/Fe_d and Fe_d/Fe_t are metrics for the crystallinity of iron bearing weathering products and, more generally, for soil development. Allophane content was estimated following from the approach described by Mizota and van Reeuwijk (1989):

$$\%Allophane = \frac{100}{\%Si_{Allo}} * \%Si_o \quad (4)$$

where $\%SI_{Allo} = -5.1 * Al_o/Si_o + 23.4$ and is based on empirical data from Parfitt and Wilson (1985).

2.7. Statistical analyses

The open source software packages R (R Foundation for Statistical Computing, http://www.R-project.org) and Rstudio (Rstudio Inc., www.rstudio.com) were used to analyze data. Pearson product moment correlation was used to test for the significance of correlations between continuous variables. Linear least squares regression models were calculated to test significant linear relationships between soil depth and biogeochemical variables.

3. Results

3.1. Carbon and nitrogen concentration

There was reasonably strong agreement of total C concentrations measured pre- and post-archiving, most samples plotted along a 1:1 line, with a few post-archive measurements slightly higher than pre-archive measurements (Supplemental Fig. 2). The C and N concentrations of the archived samples ranged from 0.1 to 8% and below detection to 0.3%, respectively. The concentrations of C and N decreased sharply with depth from the soil surface to between 50 and 100 cm, below that concentrations declined more slowly with depth (Fig. 1a and b). The C/N ratio of bulk soils also generally declined with depth. The 24 and 300 kyr soils exhibited comparatively higher C and N concentrations but otherwise, no systematic temporal patterns were apparent across the CRC soils. Three of the youngest soils (11, 24, and 60 kyr)

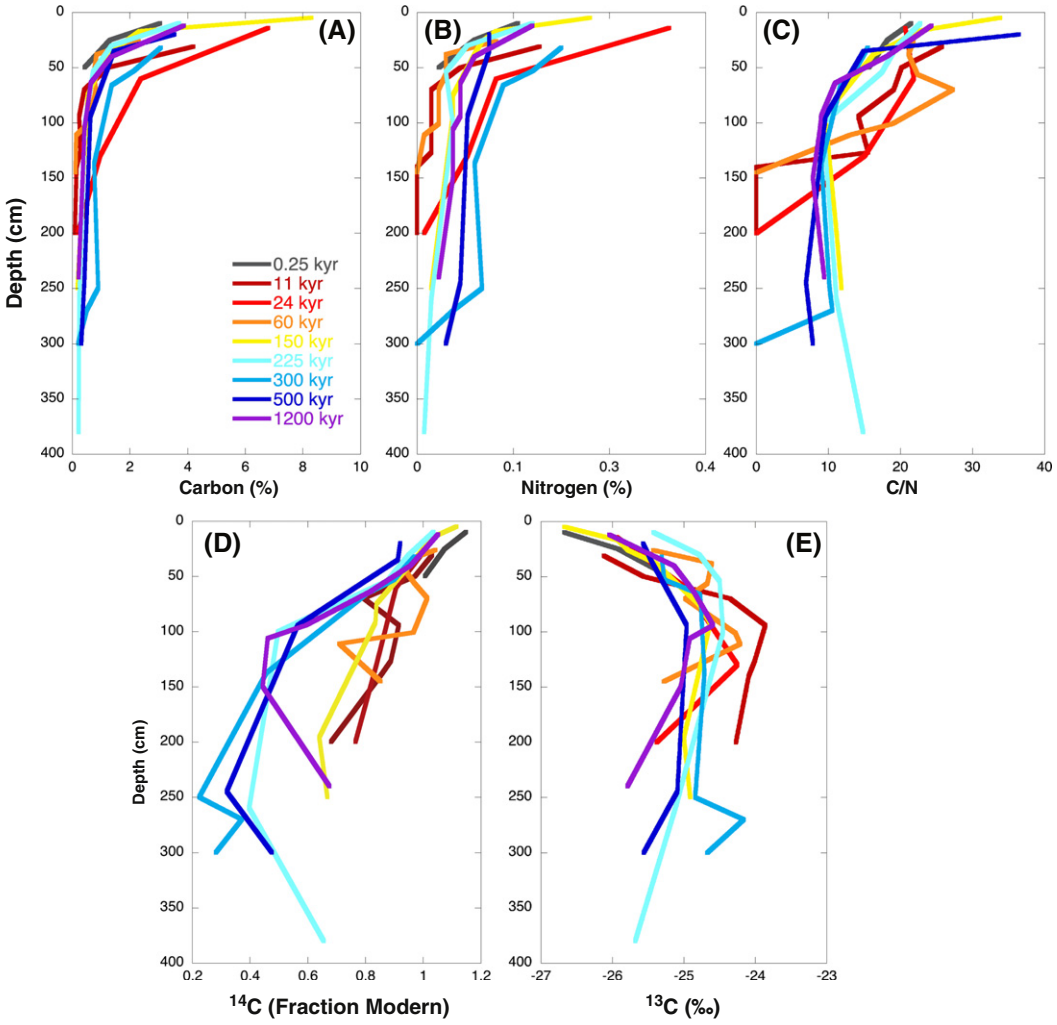

Fig. 1. Depth profiles of bulk soil (A) C concentration (%), (B) N concentration (%), (C) the C/N ratio, (D) ^{14}C isotopic composition (Fraction Modern) and (E) $\delta^{13}C$ isotopic composition (‰).

stood out with respect to C/N rations, exhibiting high values between 50 and 100 cm and decline to values near zero below that (Fig. 1c).

3.2. Carbon isotopes

Soil ^{14}C-FM content of bulk soils generally declined with increasing depth (Fig. 1d). For example, the ^{14}C-FM values decreased from 1.031 near the surface to 0.682 at depth in the 11 kyr soil. Several soil profiles exhibited slight reversals of this trend at depths below 200 cm. For instance, in the 1200 kyr soil, ^{14}C-FM decreased from 1.053 near the surface to 0.444 at 150 cm and then increased to 0.675 at 240 cm. Overall, the ^{14}C-FM profiles varied with the age of soil and the magnitude of these variations was dependent on depth (Fig. 1c). Specifically, the four oldest soils contained notably older C below 50 cm, and each these soils also exhibited age reversal (high ^{14}C-FM) in the deepest soils.

The $\delta^{13}C$ content of the archived soils ranged from −26.7 to −24.0‰ (Fig. 1e). In comparison, $\delta^{13}C$ value of contemporary surface litter at the CRC sites ranges from −29.0 to −27.4‰ (unpublished data). Bulk soil $\delta^{13}C$ values increased with increasing depth to between 50 and 100 cm, values below this depth were stable or became slightly more depleted (Fig. 1d). When $\delta^{13}C$ was plotted against ^{14}C-FM, a depth dependent threshold was apparent at approximately 50 cm (Fig. 5). Specifically, in the top 50 cm of soil profiles, values of $\delta^{13}C$ declined as ^{14}C-FM increased. At depths greater than 50 cm, there was no clear relationship between $\delta^{13}C$ and ^{14}C-FM.

3.3. Mineralogy

The youngest CRC soils were dominated by quartz (Fig. 2a) and plagioclase feldspar (Fig. 2b) but also included K-feldspar (not shown) and smectite (Fig. 2c). With increasing soil age, the amount of plagioclase decreased from approximately 40% (by volume) in the youngest soils to around 5% in the oldest (Fig. 2b). The relative abundance of quartz increased with soil age, as feldspar minerals were progressively dissolved. Similarly, the abundance of K-feldspar increased during early stages of weathering (e.g., from ~5 to a maximum of 9%) but then decreased with further soil development to values between 0 and 4%. Halloysite (Fig. 2d) and smectite (to a lesser extent) were the dominant crystalline clay minerals formed in CRC soils. Halloysite content was low in the youngest soil and increased with age, reaching values of 40 to 50% in the oldest soils (Fig. 3), reflecting the formation of a kandic horizon. Smectite increased with soil age during the first 150 kyrs of soil development, after which values plateau between 10 and 17%. Halloysite and smectite content generally increased with depth to maximum values at between 100 and 200 cm and was stable or declining below. The QXRD based estimates of clay accumulation were supported by general changes in texture measured by Dethier (1988) using physical methods (Supplemental Table 1). The QXRD data suggested only slight

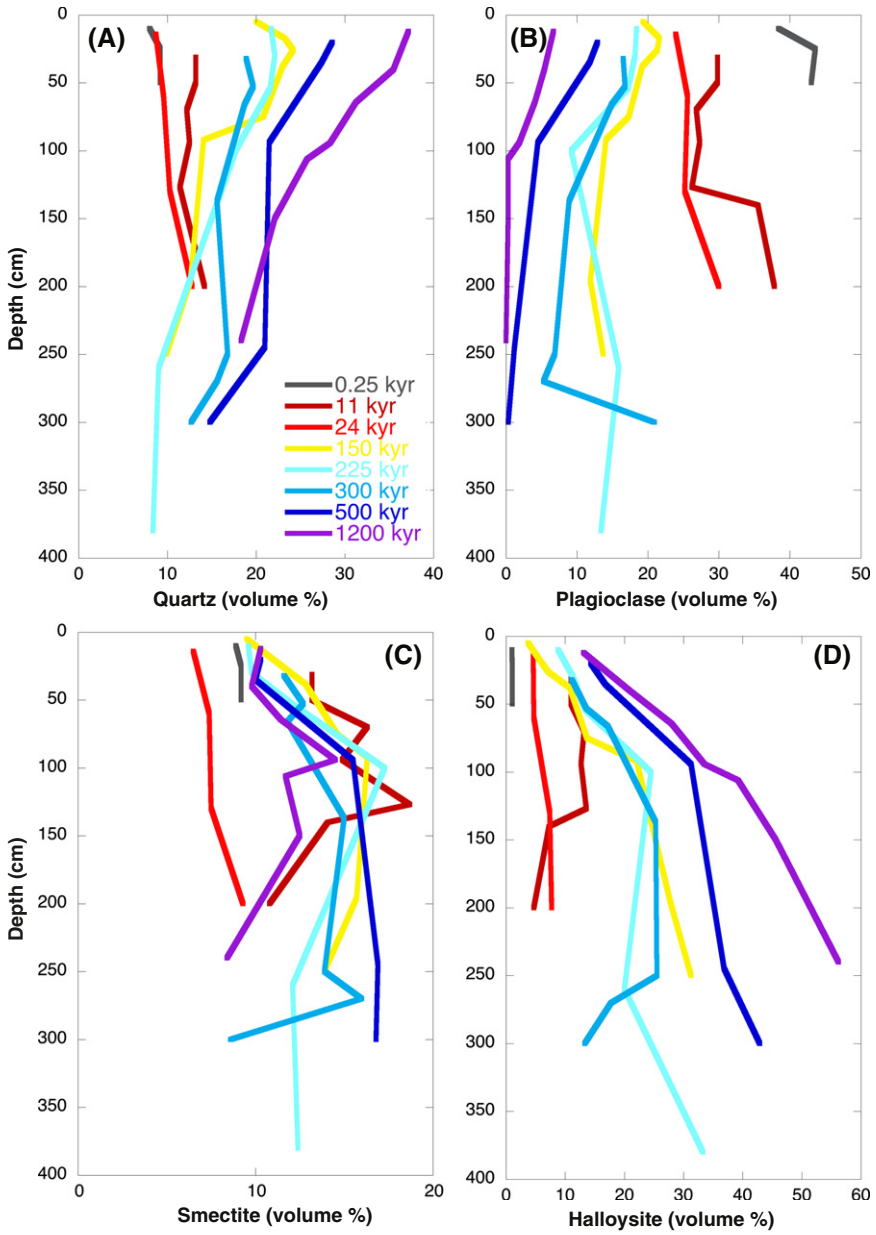

Fig. 2. Depth profiles of mineral abundances (volume %) estimated from quantitative XRD spectra following the protocols of Eberl (2003) including (A) quartz, (B) plagioclase, (D) smectite and (E) halloysite.

increases in Fe-oxides with soil development (Supplemental Table 1); however, extractable Fe_d data more clearly indicated a progressive increase with soil age (see below).

3.4. Soil elemental chemistry and chemical depletion

The major element composition of CRC soils (Supplemental Table 1) reflects long-term patterns of chemical weathering and associated changes in soil mineralogy. Mobile base cations associated with the weathering of primary minerals, including Ca, Na, K and Mg were progressively depleted (Fig. 3a). In the oldest soil (1200 kyr), between 70 and 100% of Ca, Na and K were lost via weathering fluxes. Concentrations of Si in bulk soils were also depleted through time, but losses were slower and less complete than for base cations, reaching as high as 50% Si loss in the oldest soil (Fig. 3b). In contrast, Al and Fe, were slightly enriched (negative CDF values corresponding to as much as 30% enrichment) during early stages of soil development, after which there was a progressive depletion in Fe and Al reaching as high as 50% loss in some shallow soils (Fig. 3c). In contrast to Si losses (Fig. 3b), which were constant with depth, Al and Fe losses (Fig. 3c) exhibited a depth dependency, with higher losses occurring nearer the soil surface.

3.5. Surface area

The surface area of bulk soils at the CRC ranged from 5 to 90 $m^2\ g^{-1}$ (Supplemental Table 1). Surface area was uniformly low in the youngest soils but increased with age and depth (Fig. 3d). As primary minerals were replaced by secondary clays (Fig. 3e), bulk soil surface area increased from ~5 $m^2\ g^{-1}$ in the 0.25 kyr soil to between 17 and 62 $m^2\ g^{-1}$ in the 1200 kyr soil (Fig. 3d). This was generally consistent with the transition from young soils, dominated by plagioclase and K-feldspars (0.12 to 1.48 $m^2\ g^{-1}$ (White et al., 1996)), to older soils dominated by kaolin minerals (5 to 43 $m^2\ g^{-1}$ (Dixon and Weed, 1989)). Although the CRC soils contained some very high surface area minerals, including smectite (600 to 800 $m^{-2}\ g^{-1}$ (Reid-Soukup and Ulery, 2002)) and SRO minerals such as allophane (~800 $m^2\ g^{-1}$ (Theng

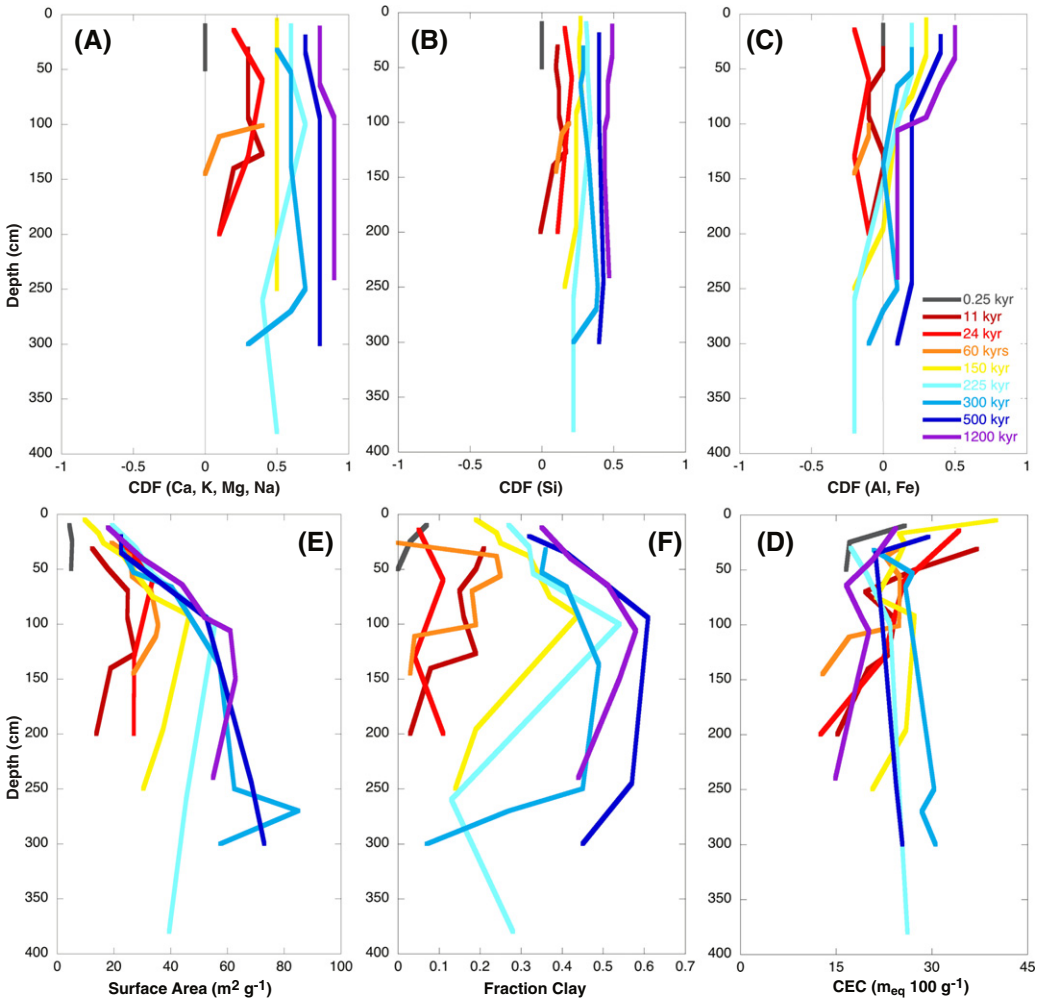

Fig. 3. Depth profiles of the chemical depletion factors (CDF) calculated for (A) the average value of mobile cations including Ca, K, Mg, and Na; (B) Si; and (C) the average value of Al and Fe. The CDF values reflect the fractional depletion (positive values) or gain (negative values) relative to an assumed starting parent material composition. Depth profiles are also plotted for (D) bulk soil surface area ($m^2\ g^{-1}$), the (E) clay fraction and (F) cation exchange capacity ($m_{eq.}\ 100\ g^{-1}$).
The fraction clay and CEC data are from Dethier (1988).

et al., 1982)), bulk soil surface areas implied that the abundance of these minerals was small. In many CRC soils, there was a pronounced change in the slope of the surface area versus depth relationship at between 50 and 100 cm. Below this depth, surface area values were relatively stable. Despite large increases in surface area with soil age, soil age dependent changes in cation exchange capacity were less clear (Fig. 3f; data from Dethier, 1988).

3.6. Soil extractions

The concentrations of Al and Fe extracted from soil samples by sequential mineral dissolution varied, but several general trends were apparent (Supplemental Table 1). Generally, extraction of soils older than 150 kyr yielded higher total Al than younger soils. Concentrations of Al extracted by each reagent decreased in the order OX > DC > PP (Fig. 4 a–c). Concentrations of Al_p ranged from 0 to 5 mg g^{-1} and decreased with depth; Al_o ranged from 2 to 30 mg g^{-1} and was stable or increased with depth; and Al_d ranged from 1 to 11 mg g^{-1} and was stable with depth. The concentration of Al_p was weakly correlated with Al_o ($r = 0.44$, $p < 0.001$) and strongly correlated with Al_d ($r = 0.76$, $p < 0.001$), Al_d was weakly correlated with Al_o. The concentrations of Fe extracted by reagents followed the order DC > OX > PP, from highest to lowest (Fig. 4 d–f). The concentrations of Fe extracted with the various reagents were not significantly correlated with one another (Table 2) but Fe_p was strongly correlated with Al_p ($r = 0.81$, $p < 0.001$) and exhibited a similar pattern with soil depth. The concentrations of Fe_d were unique in that they exhibited a clear linear increase with the soil age and were inversely correlated with the abundance of feldspar minerals and positively correlated with halloysite content (Table 2). The Si_o concentrations were strongly correlated with Al_o and Fe_o (Table 2) and were similar in magnitude to Al_o, except in some intermediate age soils (Fig. 5a).

The proportion of organo-Al was highest near the soil surface and declined rapidly with depth to around a 100 cm, below that values were relatively constant (Fig. 5b), with many of these soils exhibiting slight peaks in allophane abundance below 50 cm depth (Fig. 5c). Concentrations of allophane were highest in the 24 and 300 kyr soils, which also exhibited anomalously high concentrations of extractable metals (Si, Fe and Al) at shallow to intermediate depths (Figs. 4 and 5a). Extractable-Fe based showed variations consistent with increasing soil development (Fig. 5d–e), most notably a clear increase in the ratio Fe_d/Fe_t (Fig. 5e)

3.7. Depth integrated temporal patterns

The total amount of C stored in CRC soils (i.e., sum total profile C in units of g C cm^{-2}) varied with the age of the soil (Fig. 6a). When deep and shallow soil C stocks were considered separately, the temporal patterns were somewhat altered. Most notably, young to intermediate age soils (11 to 60 kyr) stored a greater amount of C per unit volume at

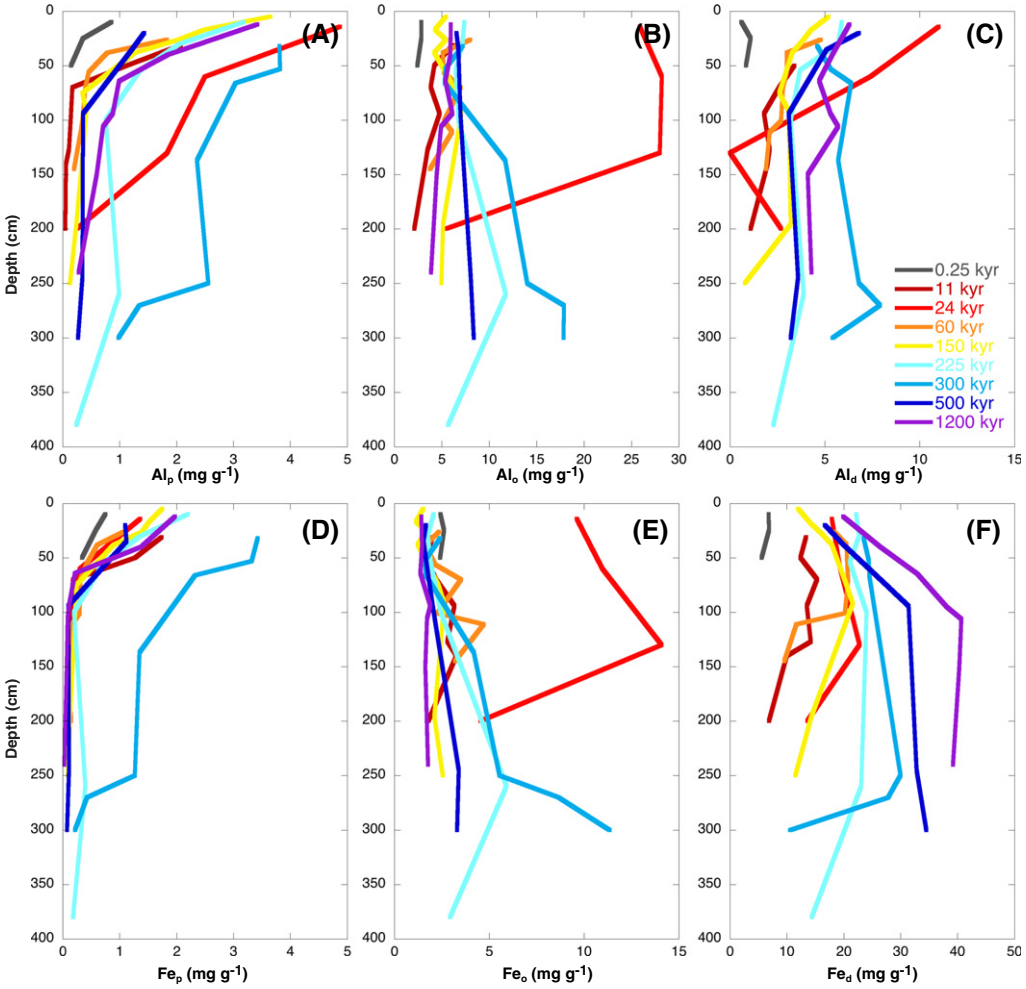

Fig. 4. Depth profiles of bulk soil sodium pyrophosphate extractable (A) Al_p and (D) Fe_p, oxalate extractable (B) Al_o and (E) Fe_p and dithionite–citrate extractable (C) Al_d and (F) Fe_p. All units are mg g^{-1}.

shallow depths (above 50 cm) compared with older soils (150 to 500 kyr), which store more C in deep soils (below 50 cm). In the 1200 kyr soil, C storage was comparable in shallow and deep soils. When soils were grouped by age, temporal variations in ^{14}C-FM were smaller in shallow versus deep soils (Fig. 5b). The mean ^{14}C-FM of organic C in soils <50 cm depth was 1.037 ± 0.025 (n = 11) and 0.990 ± 0.018 (n = 11) for ages <150 kyr and >150 kyr, respectively whereas the mean ^{14}C-FM of organic C in soils >50 cm depth was 0.837 ± 0.022 (n = 22) and 0.546 ± 0.048 (n = 18) for soil <150 kyr and >150 kyr. Declines in bulk soil ^{14}C-FM coincided with increases in surface area, particularly in deep soils (Fig. 5c). The estimated abundance of allophane was similar in deep and shallow soils throughout soil development (Fig. 5d), peaking in the 24 and 300 kyr soils. These two anomalous soils also exhibited, to varying degrees, peaks in C storage, ^{14}C-FM, surface area and Al_p (Fig. 5)

3.8. Correlations between soil physical properties with C storage and stability

Physical parameters including QXRD, extractive chemistry and surface area were compared against measured organic parameters including C and N concentrations and C isotopes (Table 2). Of the variables considered, Al_p, Fe_p and CEC were most strongly correlated with organic parameters including C, N and δ^{13}C content. In particular, the strong correlation between Al_p and C concentration was driven by a positive linear relationship (Fig. 7a). Oxalate extractable Al_o was weakly correlated with C and N concentration but was not correlated to other organic parameters, whereas extractable Fe_o was not correlated with any organic parameters. Dithionite extractable Al_d was significantly correlated with C and N content and Fe_d was correlated with ^{14}C-FM. Although Al_p was weakly correlated with ^{14}C-FM, this relationship was primarily driven by shallow soils (Fig. 7b). Surface area was inversely correlated with C/N ratio and C concentration, relationships driven primarily by deep soils (Fig. 7b), but was the variable most strongly correlated (negatively) with ^{14}C-FM (Fig. 8). When temporal trends in (depth-integrated) soil surface area were compared with ^{14}C-FM, a sharp increase bulk soil surface area in deep soils coincided with a depletion of ^{14}C (lower FM) after ~60 kyr of soil development (Fig. 8). Estimated allophane content was not strongly correlated with surface area or ^{14}C-FM (Table 2).

4. Discussion

4.1. Soil development at the CRC

Quantitative mineralogy and selective dissolution data provide insight into the temporal patterns of soil development along the CRC. Dethier (1988) recognized increases in clay and Fe_d content along with several field-based indices of soil development (especially texture and color or “rubification”), which were all correlated with relative soil ages. Additional indices of soil development reported here also closely follow the reported soil age distribution (Fig. 5d–e). These results suggest that while inputs of loess likely continued throughout the period of soil formation, inputs were not enough to reset soil development.

Table 2
Correlation coefficients for relationships between key measured data including C, N and carbon isotopes, extractive chemistry, quantitative mineralogy and physical measurements. Significance of correlations are indicated by shading where black cells corresponds to $p < 0.001$, dark-gray cells corresponds to $p < 0.01$ and light-gray cells corresponds to $p < 0.05$.

	Age	Depth	C	N	C/N	$d^{13}C$	^{14}C	CEC	SA	Al_p	Al_o	Al_d	Alp/Al_{op}	Si_o	Allop.	Fe_p	Fe_o	Fe_d	Fe_o/Fe_d	Fe_d/Fe_t	Qtz	Kspar	Plag.	Fe Ox	Halloy.	Smec.
Depth	0.10																									
C	−0.11	−0.56																								
N	−0.05	−0.54	0.92																							
C/N	−0.18	−0.57	0.61	0.45																						
$d^{13}C$	−0.04	0.31	−0.69	−0.65	−0.39																					
^{14}C	−0.34	−0.79	0.57	0.48	0.64	−0.43																				
CEC	−0.24	−0.18	0.69	0.70	0.38	−0.43	0.19																			
SA	0.49	0.65	−0.47	−0.35	−0.49	0.40	−0.86	−0.12																		
Al_p	−0.02	−0.47	0.83	0.91	0.40	−0.51	0.38	0.64	−0.27																	
Al_o	−0.17	0.04	0.29	0.34	0.16	0.07	−0.05	0.27	0.15	0.44																
Al_d	0.17	−0.22	0.56	0.65	0.30	−0.19	0.05	0.49	0.12	0.76	0.72															
Al_p/Al_{op}	0.15	−0.59	0.67	0.68	0.44	−0.56	0.46	0.44	−0.36	0.77	−0.11	0.37														
Si_o	−0.38	0.05	0.06	0.16	0.11	0.21	−0.07	0.18	0.18	0.27	0.57	0.30	−0.10													
Alloph	−0.34	0.05	0.16	0.25	0.14	0.18	−0.07	0.23	0.19	0.37	0.84	0.52	−0.13	0.92												
Fe_p	−0.02	−0.50	0.64	0.70	0.36	−0.48	0.42	0.47	−0.36	0.80	−0.04	0.38	0.91	0.06	0.01											
Fe_o	−0.27	0.19	0.09	0.11	0.02	0.19	−0.12	0.09	0.14	0.20	0.93	0.50	−0.31	0.52	0.78	−0.23										
Fe_d	0.75	0.19	−0.16	−0.01	−0.17	0.16	−0.49	−0.07	0.74	0.04	0.06	0.30	0.05	0.07	0.06	−0.03	−0.10									
Fe_o/Fe_d	−0.39	0.14	0.04	0.01	−0.10	0.06	−0.01	−0.04	−0.09	0.06	0.69	0.23	−0.35	0.30	0.53	−0.28	0.85	−0.44								
Fe_d/Fe_t	0.78	0.09	−0.14	0.02	−0.19	0.05	−0.44	−0.06	0.68	0.07	−0.07	0.27	0.17	−0.03	−0.07	0.09	−0.25	0.96	−0.55							
Qtz	0.75	−0.34	0.10	0.10	0.13	−0.13	0.02	−0.11	0.13	0.17	−0.33	0.17	0.51	−0.35	−0.39	0.34	−0.49	0.51	−0.60	0.64						
Kspar	−0.75	−0.13	0.21	0.04	0.34	−0.01	0.40	0.19	−0.55	0.15	0.14	−0.06	0.12	0.15	0.17	0.17	0.21	−0.75	0.33	−0.69	−0.34					
Plag	−0.77	−0.28	0.12	0.01	0.20	−0.02	0.56	−0.09	−0.76	−0.04	0.06	−0.27	−0.11	0.03	0.07	−0.04	0.23	−0.87	0.50	−0.89	−0.61	0.62				
FeOx	−0.08	−0.03	0.15	0.13	0.17	0.01	0.17	−0.13	−0.10	0.20	0.60	0.42	−0.18	0.25	0.45	−0.17	0.64	−0.04	0.61	−0.23	−0.32	0.01	0.25			
Halloy	0.68	0.54	−0.43	−0.33	−0.45	0.10	−0.67	−0.15	0.76	−0.35	−0.27	−0.11	−0.23	−0.18	−0.26	−0.28	−0.33	0.77	−0.49	0.74	0.30	−0.73	−0.83	−0.23		
Smec	0.04	0.35	−0.48	−0.44	−0.38	0.41	−0.44	0.06	0.42	−0.47	−0.50	−0.47	−0.23	−0.12	−0.31	−0.18	−0.48	0.24	−0.57	0.29	0.09	−0.19	−0.34	−0.66	0.45	
Clays	0.60	0.58	−0.52	−0.41	−0.50	0.24	−0.74	−0.13	0.82	−0.42	−0.31	−0.29	−0.18	−0.14	−0.24	−0.30	−0.34	0.75	−0.52	0.73	0.27	−0.69	−0.82	−0.33	0.97	0.62

Age (kyr), Depth (cm), C (carbon; %), N (nitrogen; %), $d^{13}C$ (‰), ^{14}C (fraction modern), CEC (cation exchange capacity;), SA (surface area; $m^2\ g^{-1}$), Al_p ($mg\ g^{-1}$), Al_o ($mg\ g^{-1}$), Al_d ($mg\ g^{-1}$), Si_o ($mg\ g^{-1}$), Allop. (allophane; wt. %), Fe_p ($mg\ g^{-1}$), Fe_o ($mg\ g^{-1}$), Fe_d ($mg\ g^{-1}$), Qtz (Quartz vol. %), Kspar (K-feldspar; vol. %), Plag. (plagioclase; vol. %), Fe Ox (Fe oxides; vol. %), Halloy (halloysite; vol. %), Smec. (smectite; vol. %) and clays (total clay content from QXRD; vol. %).

Young CRC soils (0.25 to 14 kyr) are composed primarily of feldspars with smaller amounts of quartz, smectite and secondary clays (Supplemental Table 1). With increased soil development, plagioclase and K-feldspar are depleted and replaced by secondary weathering products including organo-metal complexes (possibly with some colloidal oxyhydroxides), kaolin clay (identified here as halloysite), Fe and Al oxyhydroxides, smectite and SRO minerals (i.e., allophane and imogolite). The most striking changes in weathering products with increasing soil age were the increases of kaolin clay and crystalline Fe oxide. In comparison, organo-metal complexes (Fig. 4a), smectite (Fig. 2c) and allophane (Fig. 5c) also varied, but no long-term temporal pattern was evident. However, there were two notable peaks in allophane abundance in 24 and 300 kyr soils, also coinciding with increases in Al_p (Fig. 6). These sharp increases in estimated SRO abundance likely reflect heterogeneous inputs of glassy debris to these soils (i.e., Bethel, 1982; Dethier, 1988) and/or the presence of conditions more favorable to SRO mineral formation (discussed below). The overall changes in soil mineralogy described above occurred concomitantly with depletion of soil base cations (Fig. 3a–c) and a slight reduction in soil pH (Supplemental Table 1).

The depth patterns of weathering products observed at the CRC are consistent with the so-called "binary-composition" of andesitic soils, where the formation of organo-metal complexes limits the precipitation of secondary SRO minerals (Mizota and van Reeuwijk, 1989; Parfitt, 2009; Parfitt and Childs, 1988) through competition for dissolved Al (i.e., "anti-allophanic" effect) (Shoji et al., 1993). For example, the estimated abundance of organo-metals in CRC soils was highest near the soil surface and declined with depth (Fig. 5b), a spatial pattern that was strongly correlated with the distribution total organic C (Table 2). As the abundances of OC and organo-metals declined with depth, secondary minerals (e.g., halloysite and allophane) accumulated below 50 cm (Figs. 2 and 6), forming a thick kandic horizon. In some of the CRC soils, the depth of halloysite accumulation coincided with increases in allophane (compare Figs. 2d and 5c). We suspect these minerals have formed in place rather than forming in shallow soils and being translocated. This is consistent with other volcanic soils, where the formation of organo-metal complexes in shallow soils gives way to precipitation of secondary minerals at depths where organic inputs are low (Mizota and van Reeuwijk, 1989; Zehetner et al., 2003).

When and where secondary minerals do precipitate, the composition of those minerals is often controlled by other environmental factors. For example, Si concentrations are known to be an important control on the type of secondary minerals that precipitate in volcanic soils: at low Si concentrations allophane formation dominates, whereas at higher concentrations halloysite formation dominates (Parfitt, 2009; Parfitt et al., 1983; Singleton et al., 1989; Zehetner et al., 2003). Other factors such as soil–water flux and pH may also influence secondary mineral formation through similar controls on porewater geochemistry. In addition, continued input of dust during soil formation may play a role in setting the depth and extent of secondary weathering products. For example, small inputs of wind-blown material at the soil surface may sustain inputs of Si form chemical weathering (Lawrence et al., 2013), possibly sustaining halloysite formation at depth. These observations highlight a complex set of pedogenic interactions, which may control the spatial and temporal variations in weathering products observed in the CRC soils. In the context of SOC cycling, the formation

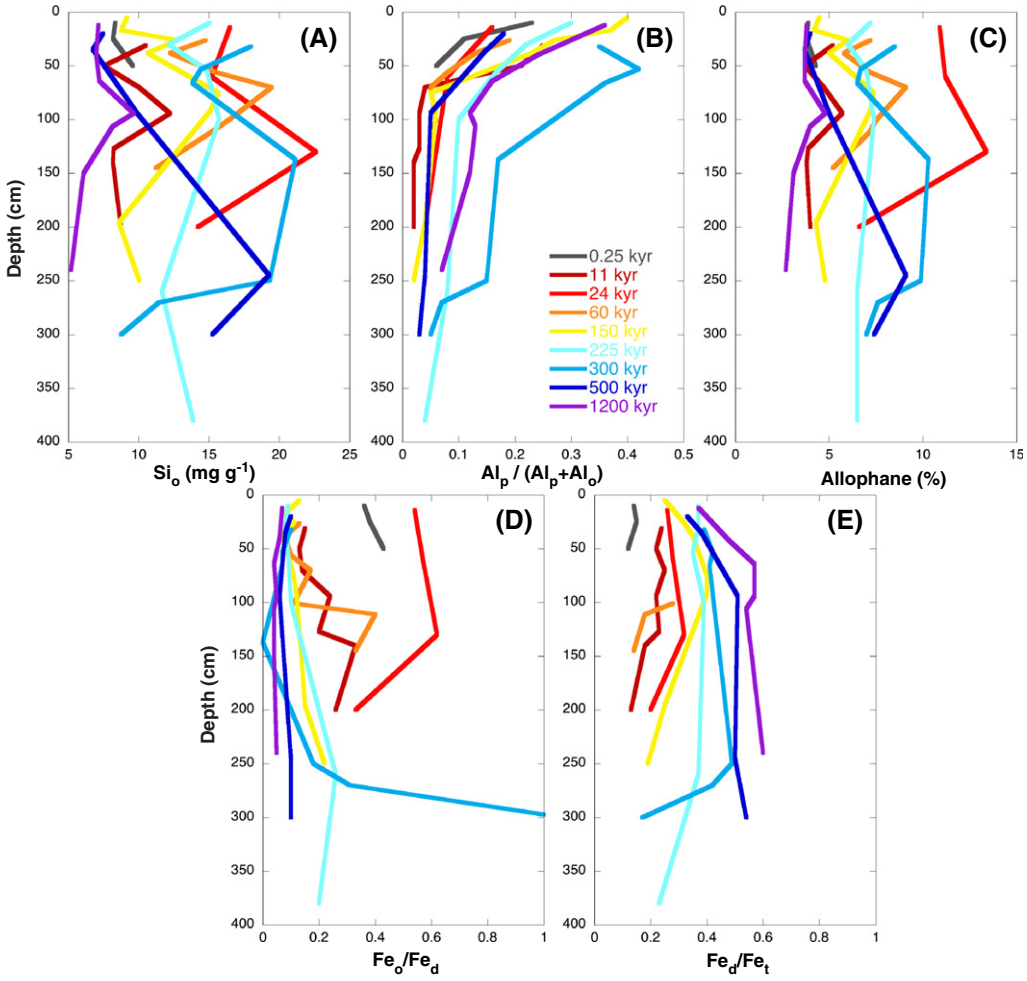

Fig. 5. Depth profiles of (A) oxalate extractable Si_o (mg g^{-1}), (B) the ratio of sodium pyrophosphate extractable Al_p to total oxalate plus pyrophosphate extractable ($Al_p + Al_o$), (C) calculated allophane content (weight %), (D) the ratio of oxalate extractable Fe_o to dithionite extractable Fe_d and (E) the ratio of dithionite extractable Fe_d to total Fe_t content.

and fate of organo-metal complexes appear to be an important control on the depth distribution of secondary minerals; however, other factors are also relevant.

4.2. Long-term controls of soil C storage and stability

Changes in SOC storage over timescales of soil development are often attributed to mineral weathering dynamics and specifically to the accumulation/transformation of secondary weathering products (Basile-Doelsch et al., 2005; Lilienfein et al., 2003; Mikutta et al., 2005; Torn et al., 1997). In the CRC soils, C and N concentrations were most strongly correlated with PP extractable Al_p and Fe_p, which are commonly used as proxies for organo-metal complexes. There is some evidence that the PP extractable metals are imperfect proxies of organo metals. For instance, Al_p is thought to be selective than Fe_p (Parfitt and Childs, 1988), which may explain stronger correlations of C and N with Al_p than with Fe_p in the CRC soils. There are also indications that PP may disperse metal-(hydr)oxide nanoparticles, leading to questions about the overall applicability of this approach for estimating organo-metals (Kaiser and Zech, 1996; Regelink et al., 2013). Given that such

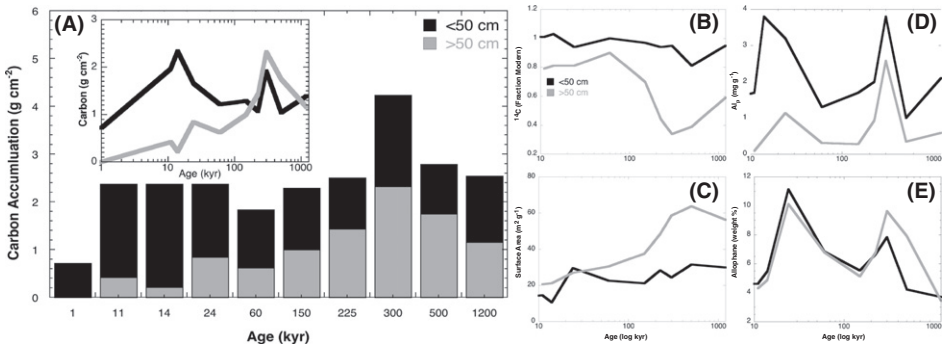

Fig. 6. Bulk soil data from the Cowlitz River Chronosequence (CRC) data are integrated over soil depth intervals from 0 to 50 cm depth (black) and >50 cm depth (gray). Variables plotted include by soil age and include (A) soil carbon content (g cm^{-2}), (B) ^{14}C content (Fraction Modern), (C) surface area (m^2 g^{-1}), sodium pyrophosphate extractable Al_p (mg g^{-1}) and (E) calculated allophane content (weight %).

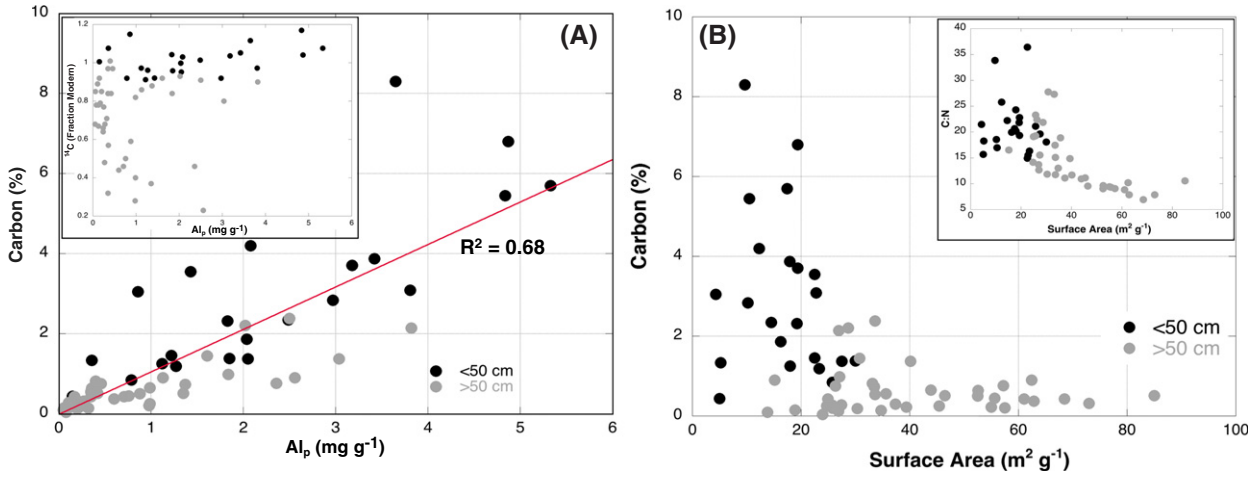

Fig. 7. (A) Sodium pyrophosphate extractable Al_p (mg g^{-1}) is plotted against bulk soil carbon concentration for and (inset) bulk soil radiocarbon content (Fraction Modern). (B) The relationships of bulk soil surface area with carbon concentration (%) and (inset) the C/N ratio of bulk soil. All data are aggregated by soil depth intervals where: <50 cm depth (black) and >50 cm depth (gray).

nanoparticles are often associated with organo-mineral complexes that are relatively mobile in soils (Regelink et al., 2011), it may be more accurate to consider the PP extractions as a proxy for mobile weathering products, including both organo-mineral nanoparticles and organo-metal complexes. Strong relationships have been observed between Al_p and SOC in Alfisols/Inceptisols/Mollisols (Masiello et al., 2004) and many other volcanic soils (Matus et al., 2008; Pena-Ramirez et al., 2009; Percival et al., 2000; Tonneijck et al., 2010). The process of organo-metal or organo-mineral complexation is thought to limit degradation of the organic components (Parfitt et al., 2002; Rasmussen et al., 2006), but the definitive cause of these widely observed correlations between Al_p and SOC remain unclear.

Storage of SOC in the CRC soils does not appear to be directly controlled by the accumulation of high-surface area secondary minerals. Though SOC and PP extractable metal concentrations were positively correlated with CEC, they were uncorrelated (e.g. allophane) or negatively correlated (e.g. surface area and clay content) with other measurements associated with secondary minerals (Table 2). These results may stem from the accumulation of organics with high surface charge and which can mask the importance of clay or other mineral surfaces (Rashidi and Seilsepour, 2008; Syers et al., 1970). The negative relationship observed between surface area and SOC content in the CRC dataset (Fig. 7b) likely results from the inverse depth patterns of SOC and clay. For example, when shallow or deep soils are considered separately the relationship is substantially weakened, a phenomenon that has also been documented in other studies (Kögel-Knabner et al., 2008). Overall, the mechanistic underpinnings of the pedogenic controls on SOC storage are elusive. Organo-metal and/or organo-mineral interactions appear to be important factors but more work is required to validate the methodologies and to determine causation of the relationships.

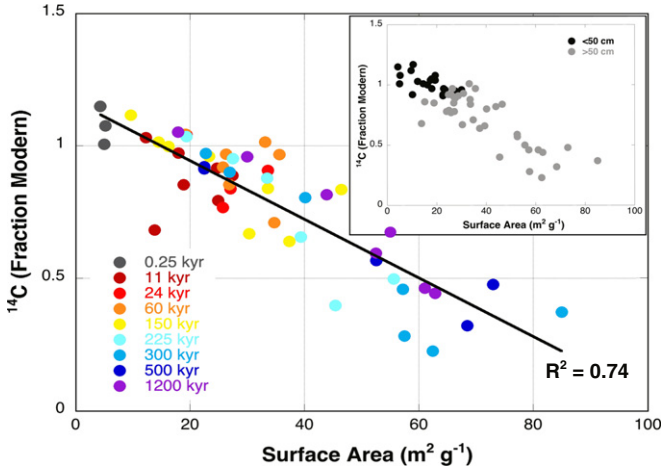

Fig. 8. Bulk soil surface area is plotted against bulk soil ^{14}C content (fraction modern) using different data categorization variables including terrace age represented using colors and (inset) soil depth intervals with <50 cm depth (black) and >50 cm depth (gray).

Soil OC stability, as interpreted from radiocarbon data, provides further insight into the interaction between soil development and SOC cycling. Generally, radiocarbon measurements of SOC at the CRC were correlated with different parameters than was total C or organo-metal proxies. Of all independent parameters considered, ^{14}C-FM was most strongly related to bulk soil surface area (Table 2). Specifically, older soil C (lower ^{14}C-FM values) was positively associated with higher surface areas (Fig. 8). Since older, more weathered soils typically exhibit the highest surface areas, it is difficult to determine whether SOC is cycling more slowly in those soils or if old soils are simply more likely to contain old C. However, the mean age of SOC (as estimated from ^{14}C) is roughly one to two orders of magnitude younger than the age of the soils (Supplemental Table 1). Thus, differences in ^{14}C-FM of SOC most likely result from differences in the rate of C turnover between soils of different ages (i.e., slower turnover of C in soils with greater surface area).

The observed increases in soil surfaces seem to result from the accumulation of kaolin clays and (to a lesser extent) smectite, as indicated by strong inverse correlations of ^{14}C-FM with those parameters (Table 2). Although allophane has a much greater surface area than halloysite, it was not significantly correlated with bulk soil surface area or ^{14}C-FM in CRC soils (Table 2). Previous work has shown soil OC stability can result from direct bonding of organics on mineral surfaces and/or through the development of soil structure, which may promote physical occlusion limiting access to SOC by microbes or even the diffusion of oxygen (Edwards and Bremner, 1967; Kleber et al., 2007; Six et al., 2004; Sollins et al., 1996; Tisdall and Oades, 1982). Consistent with these views of C stabilization, data from CRC soils suggests that the increasing age of soil C and possibly C turnover is related to the accumulation of mineral surfaces.

4.3. Depth gradients and the linkage of shallow and deep soils

The CRC data suggest the importance of depth dependent processes, which couple the soil development with long-term C cycling. It is well documented that controls on SOC turnover differ between shallow

and deep soil environments, with biologic processes dominating in shallow soils and physical protection becoming more important with increasing depth (Jobbagy and Jackson, 2000; Rumpel and Kögel-Knabner, 2010). White et al. (2012) defined a soil depth transition zone in terms of soil pore-water solute gradients, where declining elemental concentrations driven by biotic cycling (e.g., plant uptake or root exudation) intersect increasing concentrations controlled by abiotic processes (e.g., weathering). A similar definition may be applied in the context of organic matter cycling, where bulk SOC concentration and mineralogical data are used to define the transition from shallow to deep conditions. Specifically, shallow soils are characterized by sharp organic depth gradients, including decreasing SOC and N concentrations (Fig. 1a–b), reflecting declining inputs with depth; decreasing C/N ratios (Fig. 1c) and $\delta^{13}C$ (Fig. 1d) implying greater microbial processing of organic matter; and declining ^{14}C-FM values (Fig. 1e) indicating older C and possibly slower turnover. Below the transition zone, the depth dependent decline in these soil properties slows.

Looking across the CRC soils, the depth of the transition zone generally aligns with rooting depth and the zone of secondary mineral accumulation, which occur between 50 and 100 cm and do not vary appreciably as a function of terrace age (Figs. 1, 2). This pattern is consistent with the development of distinct soil horizons, the depth and extent of which are controlled by interactions between inputs (organic and/or mineral) and weathering processes. The input of "superimposed loess" (e.g., Dethier, 1988) might promote both a deepening of the transition zone, while declines in porosity of clay-rich subsoil minerals might promote a shallowing of the transition. As no significant shift in the depth of this transition was detected, other geochemical tools might be needed to unravel the role of wind-blown materials in the development of these soils.

Though it is tempting to think of shallow and deep soils as disconnected zones, the geochemical continuum is an important control on the evolution of soil properties and C cycling. For instance, formation of organo-metal complexes often occurs in shallow soils where dissolved weathering products interact with organic ligands, but the transport and transformation of these complexes can feedback on the spatial extent and intensity of weathering and soil development (Drever and Stillings, 1997; Ganor et al., 2009; Lawrence et al., 2014). Specifically, the presence of organo-metal complexes may limit the formation of secondary minerals such as allophane or halloysite in volcanic soils (Mizota and van Reeuwijk, 1989; Parfitt, 2009; Parfitt and Childs, 1988). Furthermore, as primary minerals are depleted near the surface (a process which may be slowed by dust inputs), the influence of organo-metal complexes on soil development and the depth of secondary mineral formation may change through time. For example, while the cause of ^{14}C-FM reversals observed in the 4 oldest soils (e.g., Fig. 1c) is unknown, it is plausible that the most recent accumulations of secondary mineral surfaces are occurring at the base of the observed profiles, allowing for stabilization of more modern C at those depths. The nature of this coupling between shallow and deep soil processes will depend on the movement of water through the soils, which influences chemical weathering rates as well as the flow of organic solutes and weathering products (Maher, 2010; Marin-Spiotta et al., 2011). One important implication is that long-term changes in soil C storage and stability are most apparent in deep soils (below 50 cm), where secondary weathering products accumulate (Fig. 6).

4.4. A conceptual framework for depth and time dependent evolution of SOC

From these observations a critical question arises: how are SOC storage and stability linked in the context of long-term soil development of

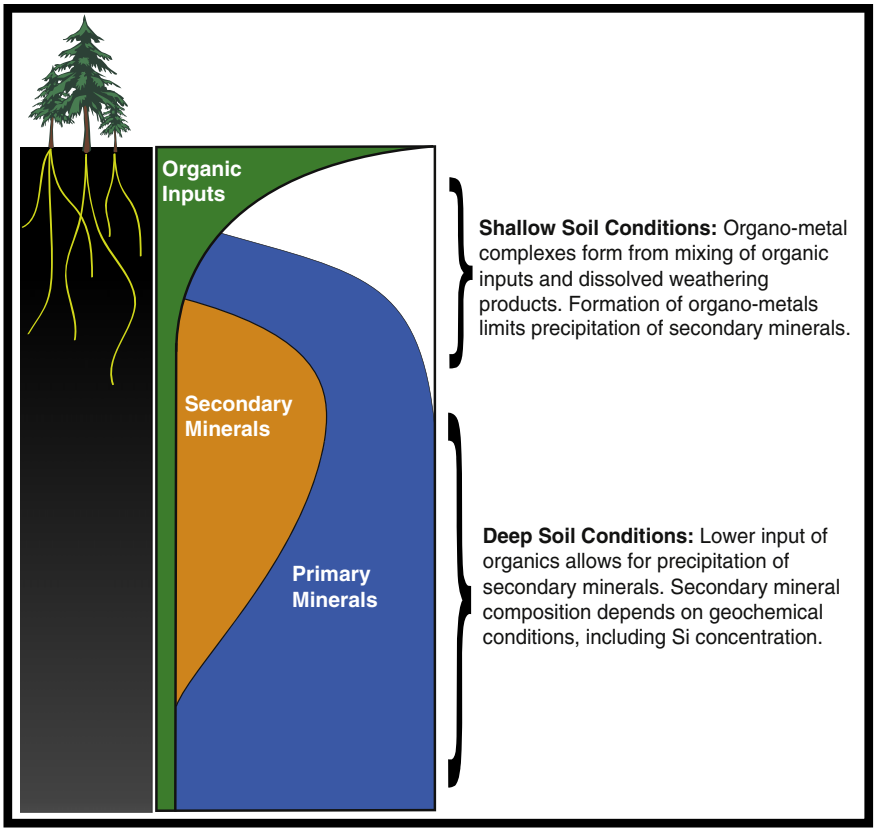

Fig. 9. A simplified conceptual framework representing the dominant processes linking soil development with carbon storage and stability in volcanic soils. In shallow soils the formation of organo-metal complexes limits precipitation of secondary minerals, whereas in deep soils limited SOC content allows precipitation of secondary minerals, the composition of which is set by other factors including the concentration of dissolved Si.

CRC soils? We propose a depth dependent framework (Fig. 9), where formation, transport and transformation of secondary weathering products are intertwined with SOC cycling. Specifically, the interaction of SOC and soil development starts in shallow soils where mobile weathering products such as organo-metal complexes (Ganor et al., 2009; Jackson, 1963; Jones, 1998; Masiello et al., 2004) or colloidal oxide/hydroxide fractions (Buettner et al., 2014) are formed. We have shown that the distribution of these weathering products is strongly correlated with SOC storage (Fig. 7); however, this relationship is not necessarily causative and C stabilized in these forms does not appear to be associated with long-term stability. More importantly, there is strong evidence that the distribution and fate of organo-metal complexes sets spatial bounds on the long-term accumulation of secondary minerals, including kaolin and SRO minerals that may have a much greater impact on C storage and stabilization.

Through the influence of secondary mineral formation, the distribution and fate of mobile weathering products explain differences in soil C storage and stability across different chronosequences. For example, the accumulation of non-crystalline SRO minerals during soil development under wet conditions resulted in enhanced SOC storage *and* stability in a Hawaiian soil age gradient (Mikutta et al., 2009; Torn et al., 1997). Soils formed from the same parent material under dryer conditions, however, do not accumulate SRO minerals to the same extent and as a result C storage is lower in those soils (Chadwick et al., 2003). Similar climate driven differences in soil secondary mineralogy and SOC content have been reported for other volcanic soils (e.g., Rasmussen et al., 2007; Zehetner et al., 2003). Although some SRO minerals do form in the CRC soils, they are not the dominant mineral influencing long-term patterns of SOC storage or stability. Instead, the progressive accumulation of kaolin minerals drives an increase in surface area, which likely provides long-term stability to a limited amount SOC. The amount of SOC stabilized in CRC soils, however, is less than in volcanic soils where SRO mineral formation is the dominant process. These variations across different soils occur as a result of complex interactions between parent material, biological inputs/processing, water flux and the resulting spatial and temporal patterns of weathering products. Over long timescales, processes such as dust deposition, vegetation and/or climate fluctuations, or even land use can influence the nature of these interactions and these processes can be challenging to reconstruct. Despite this, the broad patterns of soil development and SOC cycling observed within and between chronosequences emphasize the mechanistic underpinnings that are recorded in these datasets.

This framework of soil development highlights the complex set of factors that link soil development and C cycling in volcanic soils — but are these dynamics relevant to other soil types? Similar concepts should apply to other soils with ascending water regimes or where lateral water flow leads to horizontal soil development, and where formation of mobile weathering products, such as organo-metal complexes or colloids, influence the long-term accumulation of immobile secondary minerals. In addition to Andisols, the formation of mobile weathering products has been shown to link soil development and C cycling in Spodosols (Lundström et al., 2000) and Alfisols/Inceptisols/Mollisols (Masiello et al., 2004). In more alkaline soils, the formation of Ca complexes may be more important than Fe or Al (e.g., Oades, 1988) but similar feedbacks may still exist. In general, the applicability of this conceptual framework to different soil types can be tested through the development of new SOC models that include chemical weathering and other geochemical reactions, heterogeneous organo-mineral reactions, and transport processes. Such models will require extensive datasets, which include detailed descriptions of soil clay and amorphous mineral phases as well as quantification and isotopic characterization of organic substrates associated with various mineral phases.

Long-term chronosequence studies provide insight into the controls on SOC cycling over millennia but are also relevant to understanding C cycling over shorter timescales. For example, Kaiser and Kalbitz (2012) describe a simple conceptual model wherein depth dependent gradients of SOC age and composition are explained by a repeated sequence of retention (adsorption/desorption), microbial recycling, and transport. This concept provides a parsimonious view of many commonly observed soil properties but does not explain the depth and/or temporal variations in SOC isotopes, such as those observed at the CRC. However, when the Kaiser and Kalbitz (2012) model is combined with the conceptual framework described above, a more complete picture emerges where transport, microbial recycling, and adsorption/desorption reactions are coupled to changes in mineralogy and reactive surfaces. In this combined framework, soils at different stages of development will exhibit different secondary mineral gradients and thus, processes controlling physical exchange and biological processing of SOC will vary with soil age and depth. Although a dynamic representation of soil pedogenic processes is not required to simulate SOC patterns over shorter timescales (e.g., centuries or less), such an approach is likely better suited for understanding the coupling of biological processes (i.e., microbial mediated decomposition) with physical and chemical mechanisms of organic mater stabilization. Furthermore, the development of new modeling tools will allow for better quantification of the spatial/temporal coupling of soil development with SOC cycling and should improve predictions of soil dynamics in response to disturbance.

5. Conclusions

The CRC data described here suggest that spatial (i.e., depth) and temporal gradients in SOC storage and stability are coupled with soil weathering and progressive changes in soil mineralogy. Several conclusions can be drawn from this analysis:

1. In the CRC soils, formation of organo-metal complexes is significantly correlated with SOC storage (but not to C stability).
2. Bulk soil surface area, driven by the formation of secondary kaolin clays, was most strongly correlated with long-term stability of SOC (but not to C storage).
3. The formation of spatial and temporal biogeochemical gradients link shallow and deep soils, resulting in the development of soil structure (e.g., horizonation). These depth and age gradients may be diagnostic of processes controlling SOC cycling, particularly in deep soils.
4. Interactions of organics and mineral weathering products influence both soil development and long-term patterns of SOC cycling. Specifically, in volcanic soils, factors controlling the distribution of secondary weathering products have major impact on SOC sequestration.

Supplementary data to this article can be found online at http://dx.doi.org/10.1016/j.geoderma.2015.02.005.

Acknowledgments

Support for this work was provided by the U.S. Geological Survey Mendenhall Fellowship and Climate and Land use Mission area. The authors would like thank Alex Blum, Sasha Reed, Emily Kyker-Snowman, Meagan Mnich and Jack McFarland for their contributions including assistance in the field and laboratory and/or comments on early versions of the manuscript.

References

Amelung, W., Brodowski, S., Sandhage-Hofmann, A., Bol, R., 2008. Combining biomarker with stable isotope analyses for assessing the transformation and turnover of soil organic matter. Advances in Agronomy. Elsevier, pp. 155–250 http://dx.doi.org/10.1016/S0065-2113(08)00606-8.

Anderson, S., Dietrich, W., 2001. Chemical weathering and runoff chemistry in a steep headwater catchment. Hydrol. Process. 15, 1791–1815.

Baldock, J., Skjemstad, J., 2000. Role of the soil matrix and minerals in protecting natural organic materials against biological attack. Org. Geochem. 31, 697–710.

Basile-Doelsch, I., Amundson, R.G., Stone, W., Masiello, C.A., Bottero, J., Colin, F., Masin, F., Borschneck, D., Meunier, J., 2005. Mineralogical control of organic carbon dynamics in a volcanic ash soil on La Reunion. Eur. J. Soil Sci. 56, 689–703. http://dx.doi.org/10.1111/j.1365-2389.2005.00703.x.

Batjes, N.H., 1996. Total carbon and nitrogen in the soils of the world. Eur. J. Soil Sci. 47, 151–163.
Berggren, D., Mulder, J., 1995. The role of organic matter in controlling aluminum solubility in acidic mineral soil horizons. Geochim. Cosmochim. Acta 59, 4167–4180.
Bethel, J.P., 1982. An Investigation of the Primary and Secondary Mineralogy of a Sequence of Glacial Outwash Terraces along the Cowlitz River, Lewis County, Washington. University of Washington, Seattle.
Blanco-Canqui, H., Lal, R., 2004. Mechanisms of carbon sequestration in soil aggregates. Crit. Rev. Plant Sci. 23, 481–504. http://dx.doi.org/10.1080/07352680490886842.
Brimhall, G., Dietrich, W., 1987. Constitutive mass balance relations between chemical-composition, volume, density, porosity, and strain in metasomatic hydrochemical systems — results on weathering and pedogenesis. Geochim. Cosmochim. Acta 51, 567–587.
Brimhall, G., Chadwick, O.A., Lewis, C.J., Compston, W., Williams, I.S., Danti, K.J., Dietrich, W., Power, M.E., Hendricks, D.M., Bratt, J., 1992. Deformational mass-transport and invasive processes in soil evolution. Science 255, 695–702.
Buettner, S.W., Kramer, M.G., Chadwick, O.A., Thompson, A., 2014. Mobilization of colloidal carbon during iron reduction in basaltic soils. Geoderma 221–222, 139–145. http://dx.doi.org/10.1016/j.geoderma.2014.01.012.
Chadwick, O.A., Chorover, J., 2001. The chemistry of pedogenic thresholds. Geoderma 100, 321–353.
Chadwick, O.A., Gavenda, R.T., Kelly, E.F., Ziegler, K., Olson, C.G., Elliott, W.C., Hendricks, D.M., 2003. The impact of climate on the biogeochemical functioning of volcanic soils. Chem. Geol. 202, 195–223. http://dx.doi.org/10.1016/j.chemgeo.2002.09.001.
Chorover, J., Amistadi, M., Chadwick, O.A., 2004. Surface charge evolution of mineral-organic complexes during pedogenesis in Hawaiian basalt. Geochim. Cosmochim. Acta 68, 4859–4876. http://dx.doi.org/10.1016/j.gca.2004.06.005.
Cusack, D., Chadwick, O.A., Hockaday, W.C., 2012. Mineralogical controls on soil black carbon preservation. Global Biogeochem. Cycles http://dx.doi.org/10.1029/2011GB004109.
Dethier, D.P., 1988. The Soil Chronosequence Along the Cowlitz River, Washington. (No. 1590-F). U.S. Geological Survey.
Dijkstra, F., Fitzhugh, R., 2003. Aluminum solubility and mobility in relation to organic carbon in surface soils affected by six tree species of the northeastern United States. Geoderma 114, 33–47.
Dixon, J.B., Weed, S.B., 1989. Kaolin and serpentine group minerals. Minerals in Soil Environments. SSSA, Madison, WI, pp. 467–525.
Drever, J., Stillings, L.L., 1997. The role of organic acids in mineral weathering. Colloids Surf. A Physicochem. Eng. Asp. 120, 167–181.
Eberl, D.D., 2003. User Guide to RockJock: A Program for Determining Quantitative Mineralogy from X-ray Diffraction Data. (No. OFR 03–78). U.S. Geological Survey, Washington.
Edwards, A.P., Bremner, J.M., 1967. Microaggregates in soils. J. Soil Sci. 18, 64–73. http://dx.doi.org/10.1111/j.1365-2389.1967.tb01488.x.
Eusterhues, K., Rumpel, C., Kleber, M., Kögel-Knabner, I., 2003. Stabilisation of soil organic matter by interactions with minerals as revealed by mineral dissolution and oxidative degradation. Org. Geochem. 34, 1591–1600. http://dx.doi.org/10.1016/j.orggeochem.2003.08.007.
Fontaine, S., Barot, S., Barre, P., Bdioui, N., Mary, B., Rumpel, C., 2007. Stability of organic carbon in deep soil layers controlled by fresh carbon supply. Nature 450, 277–281. http://dx.doi.org/10.1038/nature06275.
Ganor, J., Reznik, I.J., Rosenberg, Y.O., 2009. Organics in water–rock interactions. Rev. Mineral. Geochem. 70, 259–369. http://dx.doi.org/10.2138/rmg.2009.70.7.
Guggenberger, G., Kaiser, K., 2003. Dissolved organic matter in soil: challenging the paradigm of sorptive preservation. Geoderma 113, 293–310. http://dx.doi.org/10.1016/S0016-7061(02)00366-X.
Harden, J.W., 1982. A quantitative index of soil development from field descriptions: examples from a chronosequence in central California. Geoderma 28, 1–28.
Harden, J.W., Taylor, E.M., 1983. A quantitative comparison of soil development in 4 climatic regimes. Quat. Res. 20, 342–359. http://dx.doi.org/10.1016/0033-5894(83)90017-0.
Harden, J.W., Koven, C.D., Ping, C.-L., Hugelius, G., Mcguire, A.D., Camill, P., Jorgenson, T., Kuhry, P., Michaelson, G.J., O'Donnell, J.A., Schuur, E.A.G., Tarnocai, C., Johnson, K., Grosse, G., 2012. Field information links permafrost carbon to physical vulnerabilities of thawing. Geophys. Res. Lett. 39. http://dx.doi.org/10.1029/2012GL051958.
Huggett, R., 1998. Soil chronosequences, soil development, and soil evolution: a critical review. Catena 32, 155–172.
Jackson, M.L., 1963. Aluminum bonding in soils: a unifying principle in soil science1. Soil Sci. Soc. Am. J. 27, 1. http://dx.doi.org/10.2136/sssaj1963.03615995002700010008x.
Jackson, M.L., Tyler, S.A., Willis, A.L., Bourbeau, G.A., Pennington, R.P., 1948. Weathering sequence of clay-size minerals in soils and sediments. I. Fundamental generalizations. J. Phys. Chem. 52, 1237–1260. http://dx.doi.org/10.1021/j150463a015.
Jenny, H., 1994. Factors of Soil Formation: A System of Quantitative Pedology. Dover Publications, INC., New York.
Jobbagy, E.G., Jackson, R.B., 2000. The vertical distribution of soil organic carbon and its relation to climate and vegetation. Ecol. Appl. 10, 423–436.
Jones, D.L., 1998. Organic acids in the rhizosphere — a critical review. Plant Soil 205, 25–44. http://dx.doi.org/10.1023/a:1004356007312.
Kaiser, K., Guggenberger, G., 2000. The role of DOM sorption to mineral surfaces in the preservation of organic matter in soils. Org. Geochem. 31, 711–725.
Kaiser, K., Kalbitz, K., 2012. Cycling downwards — dissolved organic matter in soils. Soil Biol. Biochem. 52, 29–32. http://dx.doi.org/10.1016/j.soilbio.2012.04.002.
Kaiser, K., Zech, W., 1996. Defects in the estimation of aluminum in humus complexes of podzolic soils by pyrophosphate extraction. Soil Sci. 161, 452–458.
Kalbitz, K., Kaiser, K., 2008. Contribution of dissolved organic matter to carbon storage in forest mineral soils. J. Plant Nutr. Soil Sci. 171, 52–60.
Kalbitz, K., Solinger, S., Park, J., Michalzik, B., Matzner, E., 2000. Controls on the dynamics of dissolved organic matter in soils: a review. Soil Sci. 165, 277–304.
Kleber, M., Mikutta, R., Torn, M., Jahn, R., 2005. Poorly crystalline mineral phases protect organic matter in acid subsoil horizons. Eur. J. Soil Sci. 56, 717–725.
Kleber, M., Sollins, P., Sutton, R., 2007. A conceptual model of organo-mineral interactions in soils: self-assembly of organic molecular fragments into zonal structures on mineral surfaces. Biogeochemistry 85, 9–24. http://dx.doi.org/10.1007/s10533-007-9103-5.
Kögel-Knabner, I., Guggenberger, G., Kleber, M., Kandeler, E., Kalbitz, K., Scheu, S., Eusterhues, K., Leinweber, P., 2008. Organo-mineral associations in temperate soils: Integrating biology, mineralogy, and organic matter chemistry. J. Plant Nutr. Soil Sci. 171, 61–82. http://dx.doi.org/10.1002/jpln.200700048.
Lawrence, C., Reynolds, R.L., Ketterer, M.E., Neff, J.C., 2013. Aeolian controls of soil geochemistry and weathering fluxes in high-elevation ecosystems of the Rocky Mountains, Colorado. Geochim. Cosmochim. Acta 107, 27–46. http://dx.doi.org/10.1016/j.gca.2012.12.023.
Lawrence, C., Harden, J.W., Maher, K., 2014. Modeling the influence of organic acids on soil weathering. Geochim. Cosmochim. Acta 139, 487–507. http://dx.doi.org/10.1016/j.gca.2014.05.003.
Lilienfein, J., Qualls, R., Uselman, S., Bridgham, S., 2003. Soil formation and organic matter accretion in a young andesitic chronosequence at Mt. Shasta, California. Geoderma 116, 249–264. http://dx.doi.org/10.1016/S0016-7061(03)00086-7.
Loeppert, R.H., Inskeep, W.P., 1996. Iron. In: Sparks, D.L (Ed.), Methods of soil analyses: Chemical Methods (Vol. 3, pp. 639–664). Soil Science Society of America, Inc, Madison, WI.
Lundström, U.S., Van Breemen, N., Bain, D., 2000. The podzolization process. A review. Geoderma 94, 91–107.
Maher, K., 2010. The dependence of chemical weathering rates on fluid residence time. Earth Planet. Sci. Lett. 1–10. http://dx.doi.org/10.1016/j.epsl.2010.03.010.
Marin-Spiotta, E., Chadwick, O.A., Kramer, M., Carbone, M.S., 2011. Carbon delivery to deep mineral horizons in Hawaiian rain forest soils. J. Geophys. Res. 116 (G3), G03011. http://dx.doi.org/10.1029/2010JG001587.
Marschner, B., Brodowski, S., Dreves, A., 2008. How relevant is recalcitrance for the stabilization of organic matter in soils? J. Plant Nutr. Soil Sci. 171, 91–110.
Masiello, C.A., Chadwick, O.A., Southon, J., Torn, M., Harden, J.W., 2004. Weathering controls on mechanisms of carbon storage in grassland soils. Global Biogeochem. Cycles 18, GB4023. http://dx.doi.org/10.1029/2004GB002219.
Matus, F., Amigo, X., Kristiansen, S.M., 2006. Aluminium stabilization controls organic carbon levels in Chilean volcanic soils. Geoderma 132, 158–168. http://dx.doi.org/10.1016/j.geoderma.2005.05.005.
Matus, F., Garrido, E., Sepulveda, N., Carcamo, I., Panichini, M., Zagal, E., 2008. Relationship between extractable Al and organic C in volcanic soils of Chile. Geoderma 148, 180–188. http://dx.doi.org/10.1016/j.geoderma.2008.10.004.
McFadden, L.D., Weldon, R.J., 1987. Rates and processes of soil development on Quaternary terraces in Cajon Pass, California. Geol. Soc. Am. Bull. 98, 280–293.
McKeague, J.A., Day, J.H., 1966. Dithionite- and oxalate-extractable Fe and Al as Aids in differentiating various classes of soils. Can. J. Soil Sci. 46, 13–22. http://dx.doi.org/10.4141/cjss66-003.
Merrill, G.P., 1897. A Treatise on Rocks, Rock Weathering and Soils. Macmillan Company.
Mikutta, R., Kleber, M., Jahn, R., 2005. Poorly crystalline minerals protect organic carbon in clay subfractions from acid subsoil horizons. Geoderma 128, 106–115. http://dx.doi.org/10.1016/j.geoderma.2004.12.018.
Mikutta, R., Kleber, M., Torn, M., Jahn, R., 2006. Stabilization of soil organic matter: association with minerals or chemical recalcitrance? Biogeochemistry 77, 25–56. http://dx.doi.org/10.1007/s10533-005-0712-6.
Mikutta, R., Schaumann, G.E., Gildemeister, D., Bonneville, S., Kramer, M.G., Chorover, J., Chadwick, O.A., Guggenberger, G., 2009. Biogeochemistry of mineral-organic associations across a long-term mineralogical soil gradient (0.3–4100 kyr), Hawaiian Islands. Geochim. Cosmochim. Acta 73, 2034–2060. http://dx.doi.org/10.1016/j.gca.2008.12.028.
Mizota, C., van Reeuwijk, L.P., 1989. Clay mineralogy and chemistry of soils formed in volcanic material in diverse climatic regions. Soil Monograph. International Soil Information and Reference Centre, Wageningen, Netherlands.
Oades, J.M., 1988. The retention of organic-matter in soils. Biogeochemistry 5, 35–70.
Parfitt, R.L., 2009. Allophane and imogolite: role in soil biogeochemical processes. Clay Miner. 44, 135–155. http://dx.doi.org/10.1180/claymin.2009.044.1.135.
Parfitt, R.L., Wilson, A.D., 1985. Estimation of allophane and halloysite in three sequences of volcanic soils, New Zealand. In: Fernandez Caldas, E, Yaalon, D.H (Eds.), Volcanic Soils. Catena Suppl 7, 1–8.
Parfitt, R.L., Childs, C.W., 1988. Estimation of forms of Fe and Al-a review, and analysis of contrasting soils by dissolution and Mossbauer methods. Aust. J. Soil Res. 26, 121–144.
Parfitt, R.L., Russell, M., Orbell, G.E., 1983. Weathering sequence of soils from volcanic ash involving allophane and halloysite, New Zealand. Geoderma 29, 41–57. http://dx.doi.org/10.1016/0016-7061(83)90029-0.
Parfitt, R.L., Parshotam, A., Salt, G.J., 2002. Carbon turnover in two soils with contrasting mineralogy under long-term maize and pasture. Aust. J. Soil Res. 40, 127–136.
Pena-Ramirez, V.M., Vazquez-Selem, L., Siebe, C., 2009. Soil organic carbon stocks and forest productivity in volcanic ash soils of different age (1835–30,500 years BP) in Mexico. Geoderma 149, 224–234. http://dx.doi.org/10.1016/j.geoderma.2008.11.038.
Percival, H., Parfitt, R., Scott, N., 2000. Factors controlling soil carbon levels in New Zealand grasslands: is clay content important? Soil Sci. Soc. Am. J. 64, 1623–1630.
Rashidi, M., Seilsepour, M., 2008. Modeling of soil cation exchange capacity based on soil organic carbon. J. Agric. Biol. Sci. 3, 41–45.
Rasmussen, C., Torn, M., Southard, R., 2005. Mineral assemblage and aggregates control carbon dynamics in a California conifer forest. Soil Sci. Soc. Am. J. 69, 1711–1721. http://dx.doi.org/10.2136/sssaj2005.0040.

Rasmussen, C., Southard, R.J., Horwath, W.R., 2006. Mineral control of organic carbon mineralization in a range of temperate conifer forest soils. Glob. Chang. Biol. 12, 834–847. http://dx.doi.org/10.1111/j.1365-2486.2006.01132.x.

Rasmussen, C., Matsuyama, N., Dahlgren, R.A., Southard, R.J., Brauer, N., 2007. Soil genesis and mineral transformation across an environmental gradient on andesitic lahar. 71 pp. 225–237. http://dx.doi.org/10.2136/sssaj2006.0100.

Regelink, I.C., Weng, L., van Riemsdijk, W.H., 2011. The contribution of organic and mineral colloidal nanoparticles to element transport in a podzol soil. Appl. Geochem. 26, S241–S244. http://dx.doi.org/10.1016/j.apgeochem.2011.03.114.

Regelink, I.C., Weng, L., Koopmans, G.F., van Riemsdijk, W.H., 2013. Asymmetric flow field-flow fractionation as a new approach to analyse iron-(hydr)oxide nanoparticles in soil extracts. Geoderma 202–203, 134–141. http://dx.doi.org/10.1016/j.geoderma.2013.03.015.

Reid-Soukup, D.A., Ulery, A.L., 2002. Smectites. In: Dixon, J.B., Schulze, D.G. (Eds.), Soil Mineraology with Environmental Applications. Soil Science Society of America, Madison.

Riebe, C.S., Kirchner, J.W., Granger, D.E., 2001. Quantifying quartz enrichment and its consequences for cosmogenic measurements of erosion rates from alluvial sediment and regolith. Geomorphology 40, 15–19.

Rumpel, C., Kögel-Knabner, I., 2010. Deep soil organic matter—a key but poorly understood component of terrestrial C cycle. Plant Soil 338, 143–158. http://dx.doi.org/10.1007/s11104-010-0391-5.

Sanderman, J., Amundson, R.G., 2009. A comparative study of dissolved organic carbon transport and stabilization in California forest and grassland soils. Biogeochemistry 92, 41–59. http://dx.doi.org/10.1007/s10533-008-9249-9.

Sanderman, J., Baldock, J.A., Amundson, R.G., 2008. Dissolved organic carbon chemistry and dynamics in contrasting forest and grassland soils. Biogeochemistry 89, 181–198. http://dx.doi.org/10.1007/s10533-008-9211-x.

Schimel, J.P., Wetterstedt, J.Å.M., Holden, P.A., Trumbore, S.E., 2011. Drying/rewetting cycles mobilize old C from deep soils from a California annual grassland. Soil Biol. Biochem. 43, 1101–1103. http://dx.doi.org/10.1016/j.soilbio.2011.01.008.

Schmidt, M.W.I., Torn, M.S., Abiven, S., Dittmar, T., Guggenberger, G., Janssens, I.A., Kleber, M., Kögel-Knabner, I., Manning, D.A.C., Nannipieri, P., Rasse, D.P., Weiner, S., Trumbore, S.E., 2011. Persistence of soil organic matter as an ecosystem property. Nature 478, 49–56. http://dx.doi.org/10.1038/nature10386.

Schwesig, D., Kalbitz, K., Matzner, E., 2003. Effects of aluminium on the mineralization of dissolved organic carbon derived from forest floors. Eur. J. Soil Sci. 54, 311–322.

Shoji, S., Nanzyo, M., Dahlgren, R.A., 1993. Volcanic Ash Soils: Genesis, Properties and Utilization.

Singleton, P.L., Mcleod, M., Percival, H.J., 1989. Allophane and halloysite content and soil solution silicon in soils from rhyolitic volcanic material, New Zealand. Aust. J. Soil Res. 27, 67–77. http://dx.doi.org/10.1071/SR9890067.

Six, J., Elliott, E.T., Paustian, K., 2000. Soil macroaggregate turnover and microaggregate formation: a mechanism for C sequestration under no-tillage agriculture. Soil Biol. Biochem. 32, 2099–2103.

Six, J., Conant, R., Paul, E., Paustian, K., 2002. Stabilization mechanisms of soil organic matter: implications for C-saturation of soils. Plant Soil 241, 155–176.

Six, J., Bossuyt, H., Degryze, S., Denef, K., 2004. A history of research on the link between (micro) aggregates, soil biota, and soil organic matter dynamics. Soil Tillage Res. 79, 7–31. http://dx.doi.org/10.1016/j.still.2004.03.008.

Soils Survey of Lewis Country area, Washington, 1987. Soils Survey of Lewis Country area, Washington (Washington, D.C., U.S.).

Sollins, P., Homann, P., Caldwell, B., 1996. Stabilization and destabilization of soil organic matter: mechanisms and controls. Geoderma 74, 65–105.

Stuiver, M., Polach, H., 1977. Reporting of 14C data. Radiocarbon 19, 355–363.

Syers, J.K., Campbell, A.S., Walker, T.W., 1970. Contribution of organic carbon and clay to cation exchange capacity in a chronosequence of sandy soils. Plant Soil 33, 102–112.

Tarnocai, C., Canadell, J.G., Schuur, E.A.G., Kuhry, P., Mazhitova, G., Zimov, S., 2009. Soil organic carbon pools in the northern circumpolar permafrost region. Global Biogeochem. Cycles 23, GB2023. http://dx.doi.org/10.1029/2008GB003327.

Theng, B., Russell, M., Churchman, G.J., Parfitt, R.L., 1982. Surface properties of allophane, halloysite, and imogolite. Clay Clay Miner. 30, 143–149.

Tisdall, J.M., Oades, J.M., 1982. Organic matter and water-stable aggregates in soils. J. Soil Sci. 33, 141–163.

Tonneijck, F.H., Jansen, B., Nierop, K.G.J., Verstraten, J.M., Sevink, J., De Lange, L., 2010. Towards understanding of carbon stocks and stabilization in volcanic ash soils in natural Andean ecosystems of northern Ecuador. Eur. J. Soil Sci. 61, 392–405. http://dx.doi.org/10.1111/j.1365-2389.2010.01241.x.

Torn, M., Trumbore, S.E., Chadwick, O.A., Vitousek, P.M., Hendricks, D.M., 1997. Mineral control of soil organic carbon storage and turnover. Nature 389, 170–173.

Trumbore, S.E., 2009. Radiocarbon and soil carbon dynamics. Annu. Rev. Earth Planet. Sci. 37, 47–66. http://dx.doi.org/10.1146/annurev.earth.36.031207.124300.

Trumbore, S.E., Czimczik, C.I., 2008. Geology — an uncertain future for soil carbon. Science 321, 1455–1456. http://dx.doi.org/10.1126/science.1160232.

van Hees, P.A.W., Lundström, U.S., Giesler, R., 2000. Low molecular weight organic acids and their Al-complexes in soil solution — composition, distribution and seasonal variation in three podzolized soils. Geoderma 94, 173–200.

von Lützow, M., Kögel-Knabner, I., 2010. Response to the concept paper: "what is recalcitrant soil organic matter?" by Markus Kleber. Environ. Chem. 7, 333–335. http://dx.doi.org/10.1071/EN10085.

von Lützow, M., Kögel-Knabner, I., Ekschmitt, K., Matzner, E., Guggenberger, G., Marschner, B., Flessa, H., 2006. Stabilization of organic matter in temperate soils: mechanisms and their relevance under different soil conditions — a review. Eur. J. Soil Sci. 57, 426–445. http://dx.doi.org/10.1111/j.1365-2389.2006.00809.x.

Wada, K., Higashi, T., 1976. The categories of aluminium- and iron–humus complexes in ando soils determined by selective dissolution. Eur. J. Soil Sci. 27, 357–368. http://dx.doi.org/10.1111/j.1365-2389.1976.tb02007.x.

Wagai, R., Mayer, L.M., Kitayama, K., Shirato, Y., 2011. Association of organic matter with iron and aluminum across a range of soils determined via selective dissolution techniques coupled with dissolved nitrogen analysis. Biogeochemistry 112, 95–109. http://dx.doi.org/10.1007/s10533-011-9652-5.

Walker, L.R., Wardle, D.A., Bardgett, R.D., Clarkson, B.D., 2010. The use of chronosequences in studies of ecological succession and soil development. J. Ecol. 98, 725–736. http://dx.doi.org/10.1111/j.1365-2745.2010.01664.x.

White, A., Blum, A., Schulz, M., Bullen, T., Harden, J.W., Peterson, M., 1996. Chemical weathering rates of a soil chronosequence on granitic alluvium.1. Quantification of mineralogical and surface area changes and calculation of primary silicate reaction rates. Geochim. Cosmochim. Acta 60, 2533–2550.

White, A., Schulz, M.S., Vivit, D.V., Blum, A.E., Stonestrom, D.A., Anderson, S.P., 2008. Chemical weathering of a marine terrace chronosequence, Santa Cruz, California I: interpreting rates and controls based on soil concentration–depth profiles. Geochim. Cosmochim. Acta 72, 36–68. http://dx.doi.org/10.1016/j.gca.2007.08.029.

White, A., Schulz, M.S., Vivit, D.V., Bullen, T.D., Fitzpatrick, J., 2012. The impact of biotic/abiotic interfaces in mineral nutrient cycling: a study of soils of the Santa Cruz chronosequence, California. Geochim. Cosmochim. Acta 77, 62–85. http://dx.doi.org/10.1016/j.gca.2011.10.029.

Xu, X., Trumbore, S.E., Zheng, S., Southon, J.R., McDuffee, K.E., Luttgen, M., Liu, J.C., 2007. Modifying a sealed tube zinc reduction method for preparation of AMS graphite targets: reducing background and attaining high precision. Presented at the Nuclear Instruments & Methods in Physics Research Section B—Beam Interactions with Materials and Atoms, pp. 320–329 http://dx.doi.org/10.1016/j.nimb.2007.01.175.

Zehetner, F., Miller, W.P., West, L.T., 2003. Pedogenesis of volcanic ash soils in Andean Ecuador. Soil Sci. Soc. Am. J. 67, 1797. http://dx.doi.org/10.2136/sssaj2003.1797.